Electronic Supplementary Material (ESI) for Dalton Transactions.
This journal is © The Royal Society of Chemistry 2024

Electronic Supplementary Material (ESI)

Table of contents

NMR Spectroscopic Data

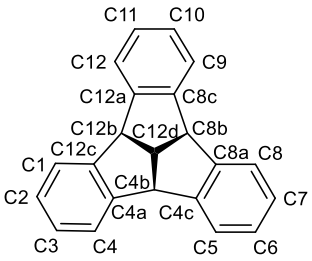

Scheme 1 Numbering scheme of tribenzotriquinacene for NMR assignments.

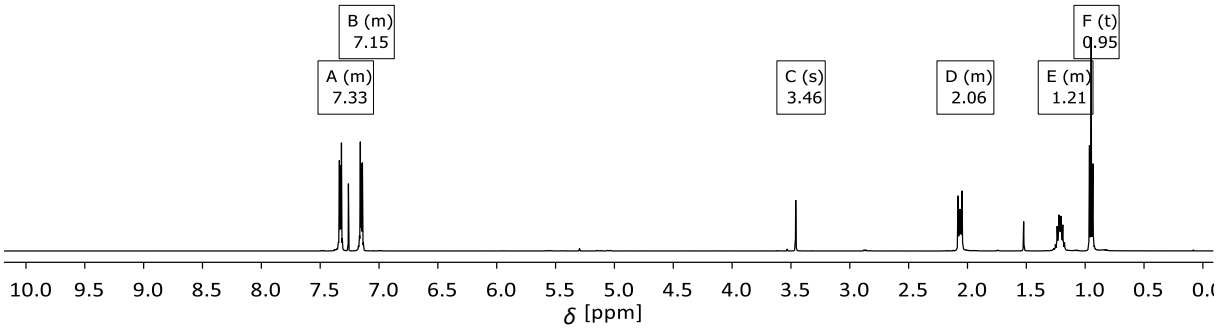

Figure S1 ^{1}H NMR spectrum of a solution of 4b,8b,12b-tri-*n*-propyltribenzotriquinacene (**2**) in $CDCl_3$ (500 MHz, 293 K).

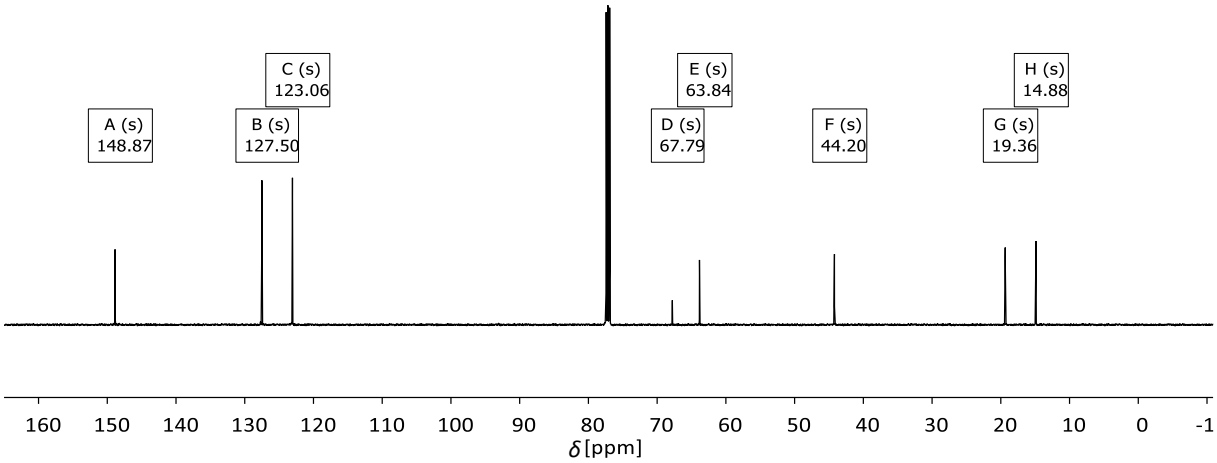

Figure S2 $^{13}C\{^{1}H\}$ NMR spectrum of a solution of 4b,8b,12b-tri-*n*-propyltribenzotriquinacene (**2**) in $CDCl_3$ (126 MHz, 293 K).

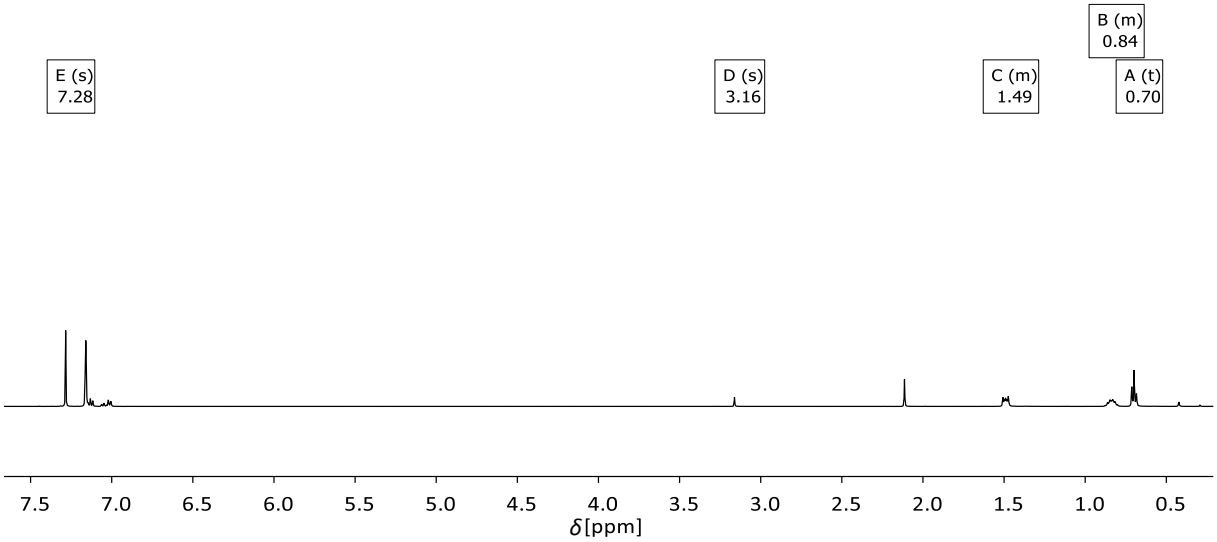

Figure S3 ^{1}H NMR spectrum 2,3,6,7,10,11-hexabromo-4b,8b,12b-tri-*n*-propyltribenzotriquinacene (**3**) in C_6D_6 (500 MHz, 293 K).

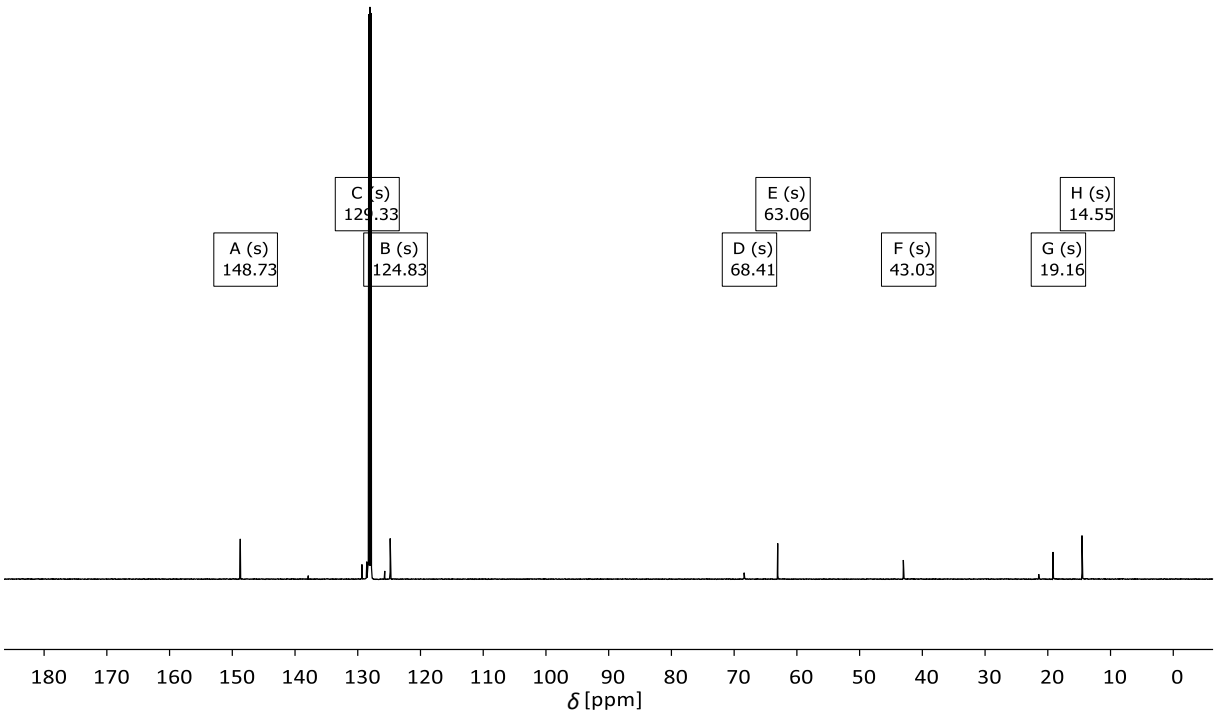

Figure S4 $^{13}C\{^{1}H\}$ NMR spectrum 2,3,6,7,10,11-hexabromo-4b,8b,12b-tri-*n*-propyltribenzotriquinacene (**3**) in C_6D_6 (126 MHz, 293 K).

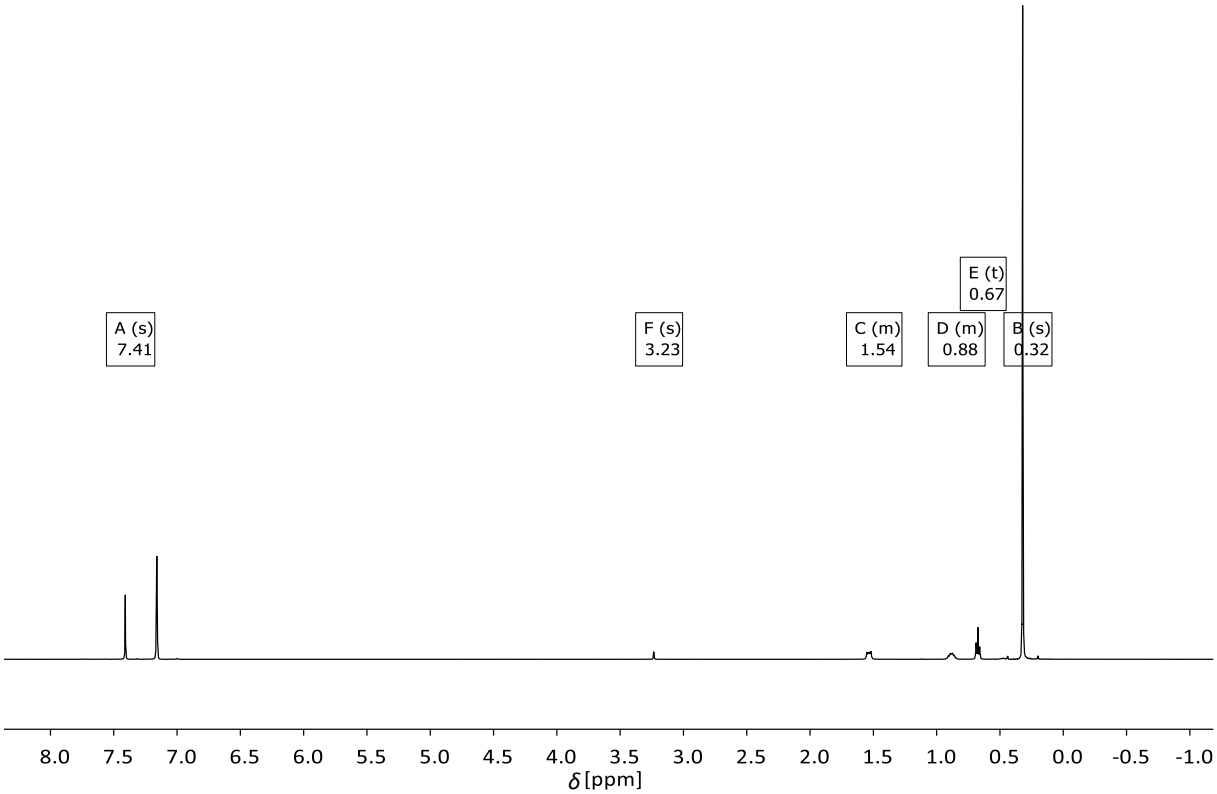

Figure S5 ^{1}H NMR spectrum of a solution of 2,3,6,7,10,11-hexakis((trimethylsilyl)ethynyl)-4b,8b,12b-tri-*n*-propyltribenzotriquinacene (**4**) in C_6D_6 (500 MHz, 293 K).

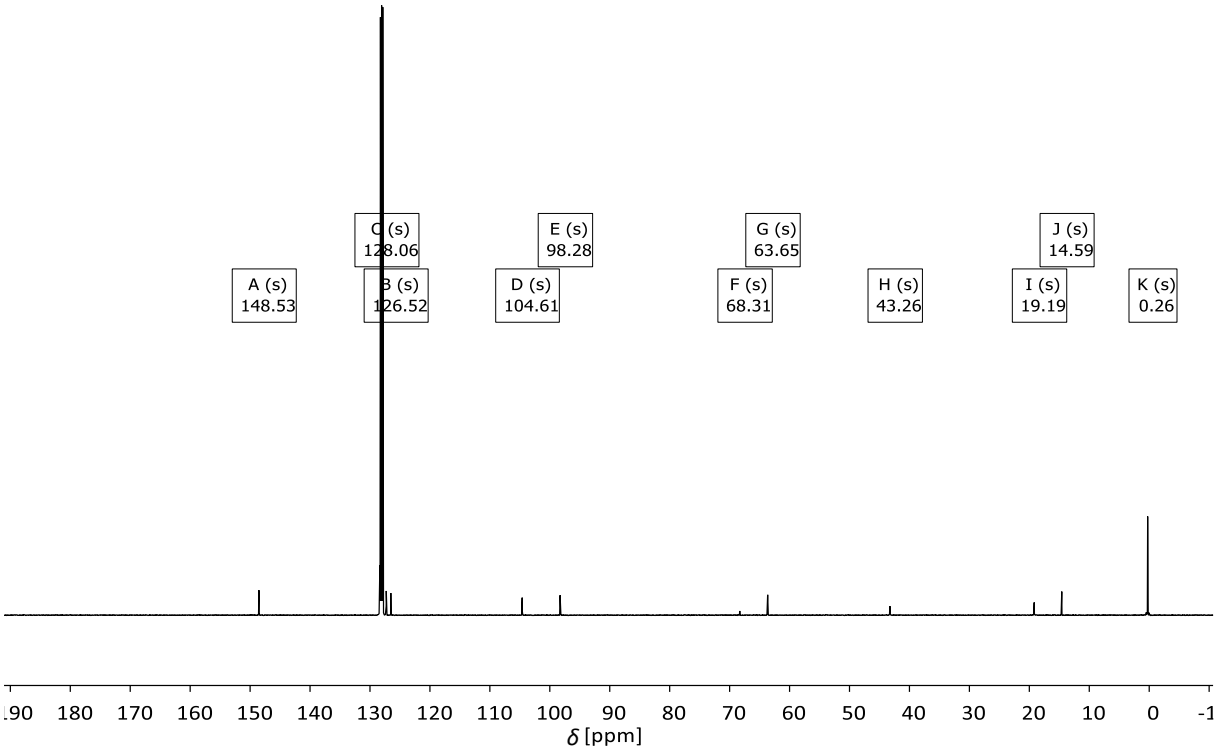

Figure S6 $^{13}C\{^{1}H\}$ NMR spectrum of a solution of 2,3,6,7,10,11-hexakis((trimethylsilyl)ethynyl)-4b,8b,12b-tripropyl-tribenzotriquinacene (**4**) in C_6D_6 (126 MHz, 293 K).

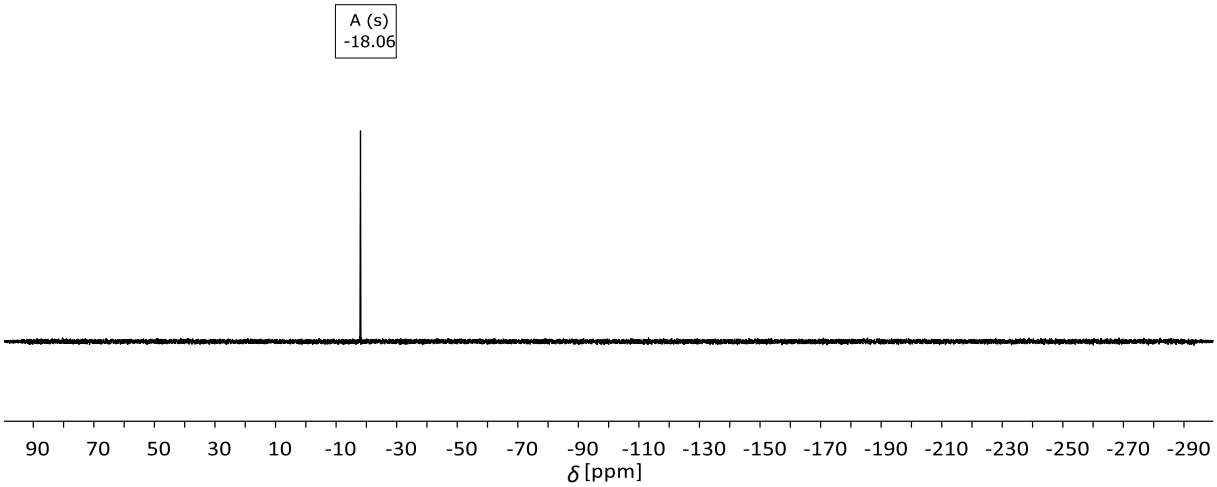

Figure S7 $^{29}Si\{^{1}H\}$ NMR spectrum of a solution of 2,3,6,7,10,11-hexakis((trimethylsilyl)ethynyl)-4b,8b,12b-tripropyl-tribenzotriquinacene (**4**) in C_6D_6 (99 MHz, 293 K).

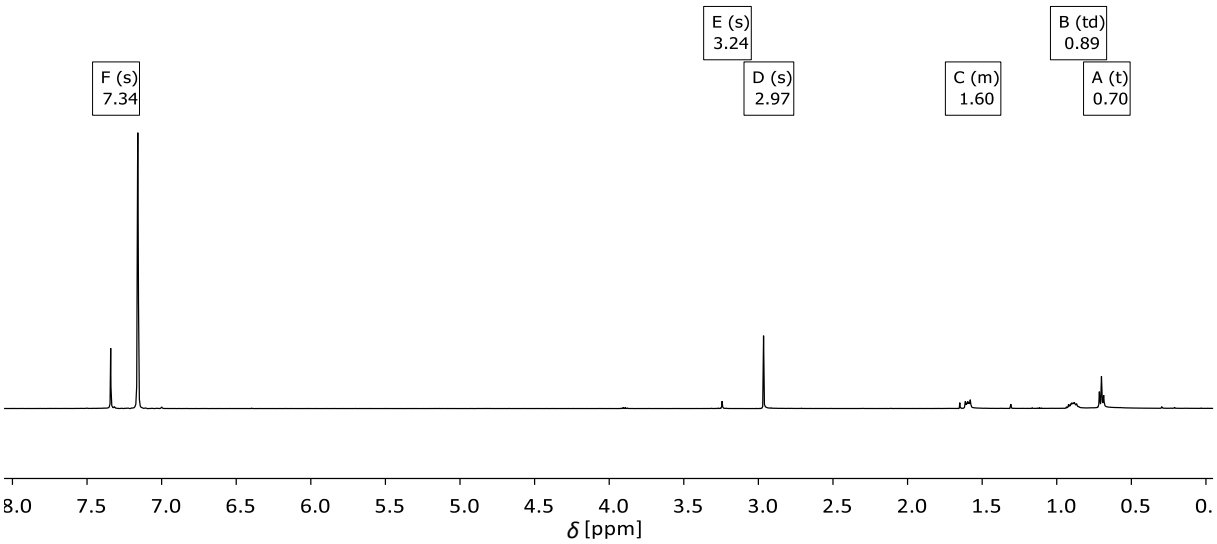

Figure S8 ^{1}H NMR spectrum of a solution of 2,3,6,7,10,11-hexaethynyl-4b,8b,12b-tri-*n*-propyltribenzotriquinacene (**5**) in C_6D_6 (500 MHz, 293 K).

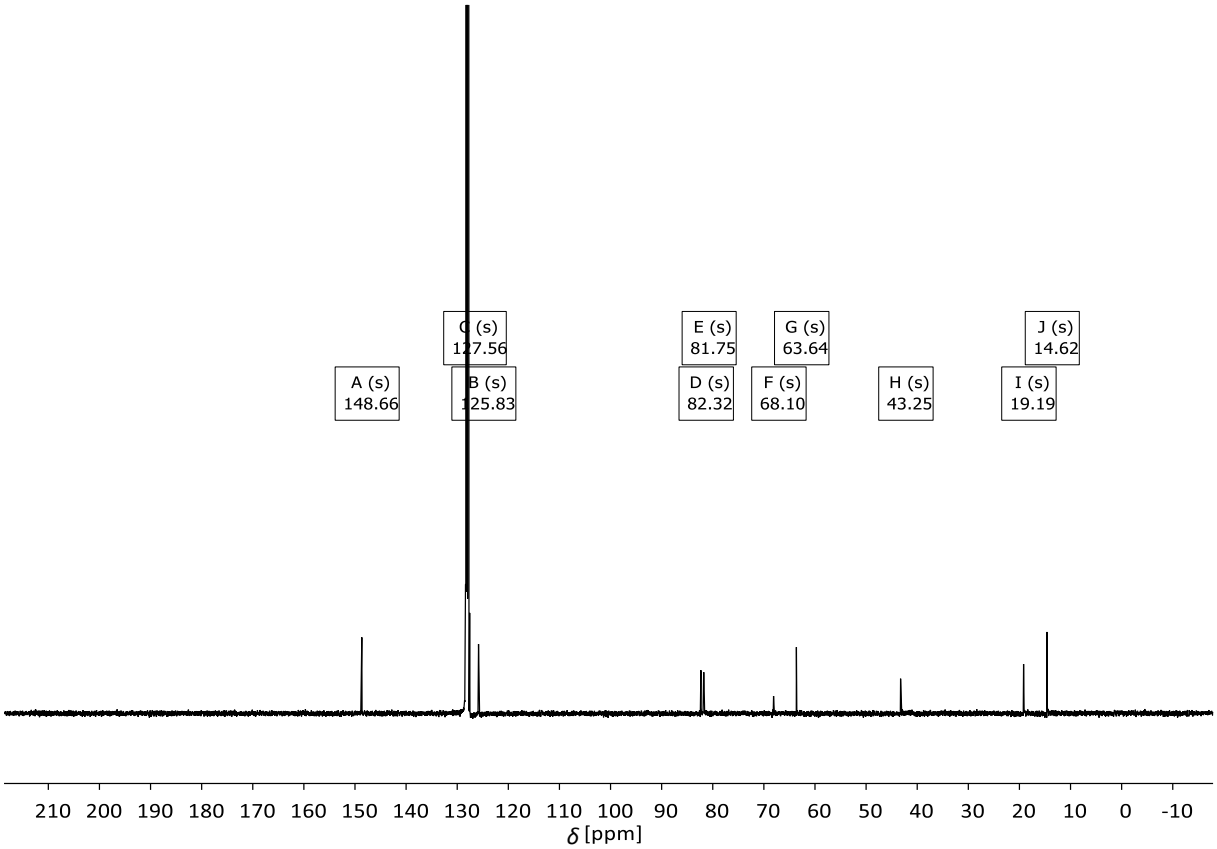

Figure S9 $^{13}C\{^{1}H\}$ NMR spectrum of a solution of 2,3,6,7,10,11-hexaethynyl-4b,8b,12b-tri-*n*-propyltribenzotriquinacene (**5**) in C_6D_6 (126 MHz, 293 K).

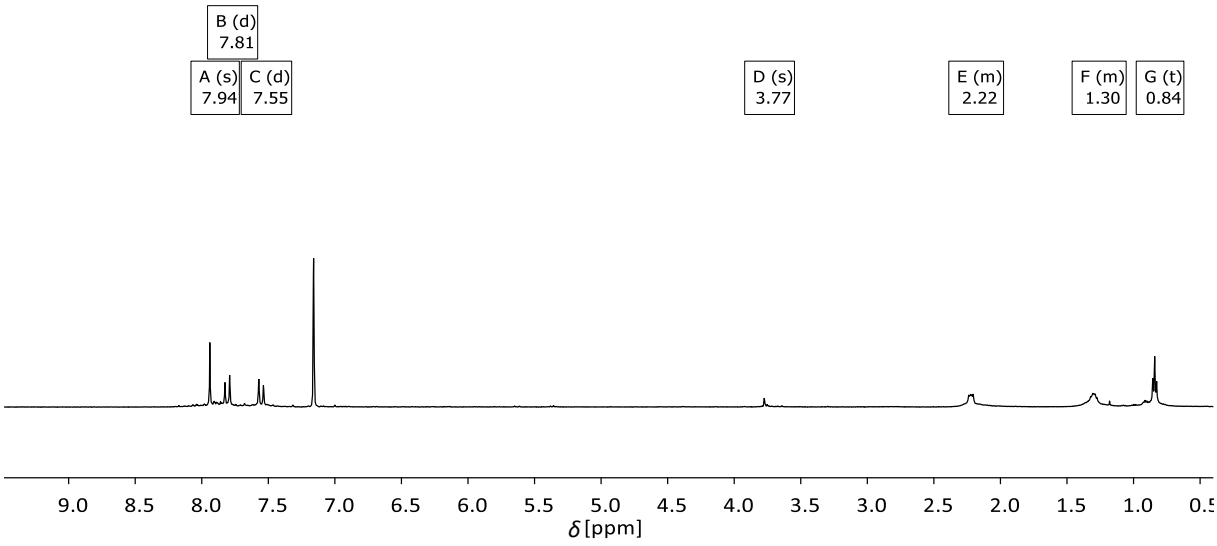

Figure S10 ^{1}H NMR spectrum of a solution of 2,3,6,7,10,11-hexakis(bis(pentafluorophenyl)boryl)vinyl-4b,8b,12b-tri-*n*-propyl-tribenzotriquinacene (**6**) in C_6D_6 (500 MHz, 293 K).

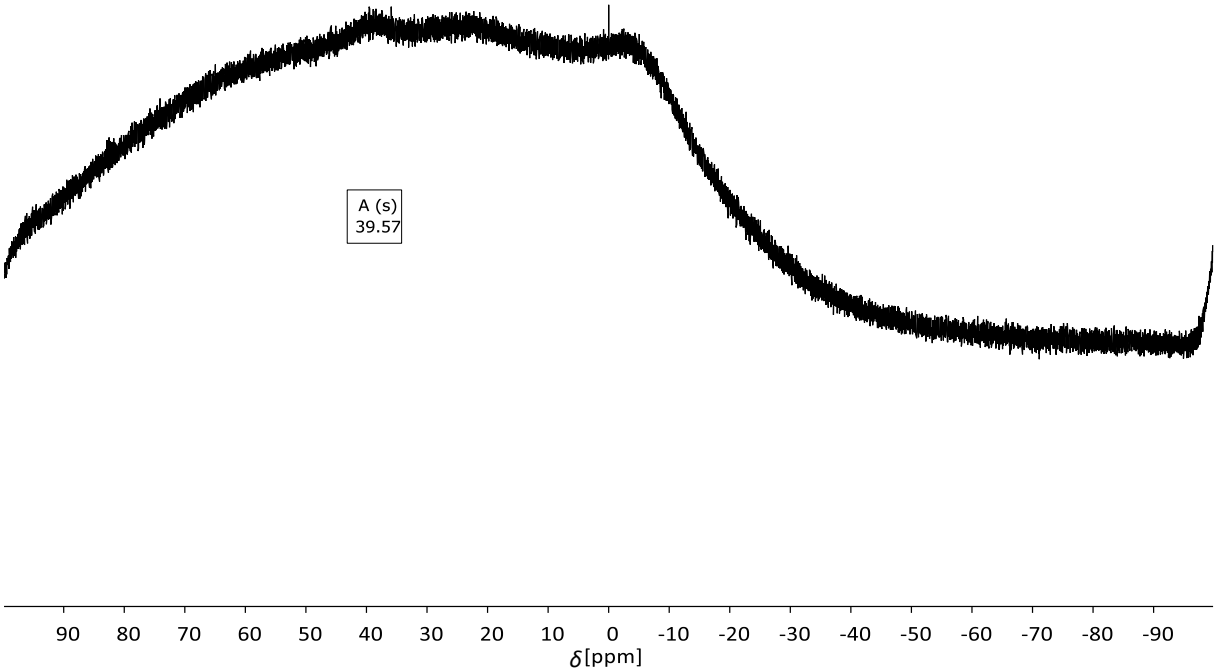

Figure S11 ^{11}B NMR spectrum of a solution of 2,3,6,7,10,11-hexakis(bis(pentafluorophenyl)boryl)vinyl-4b,8b,12b-tri-*n*-propyl-tribenzotriquinacene (**6**) in C_6D_6 (126 MHz, 293 K).

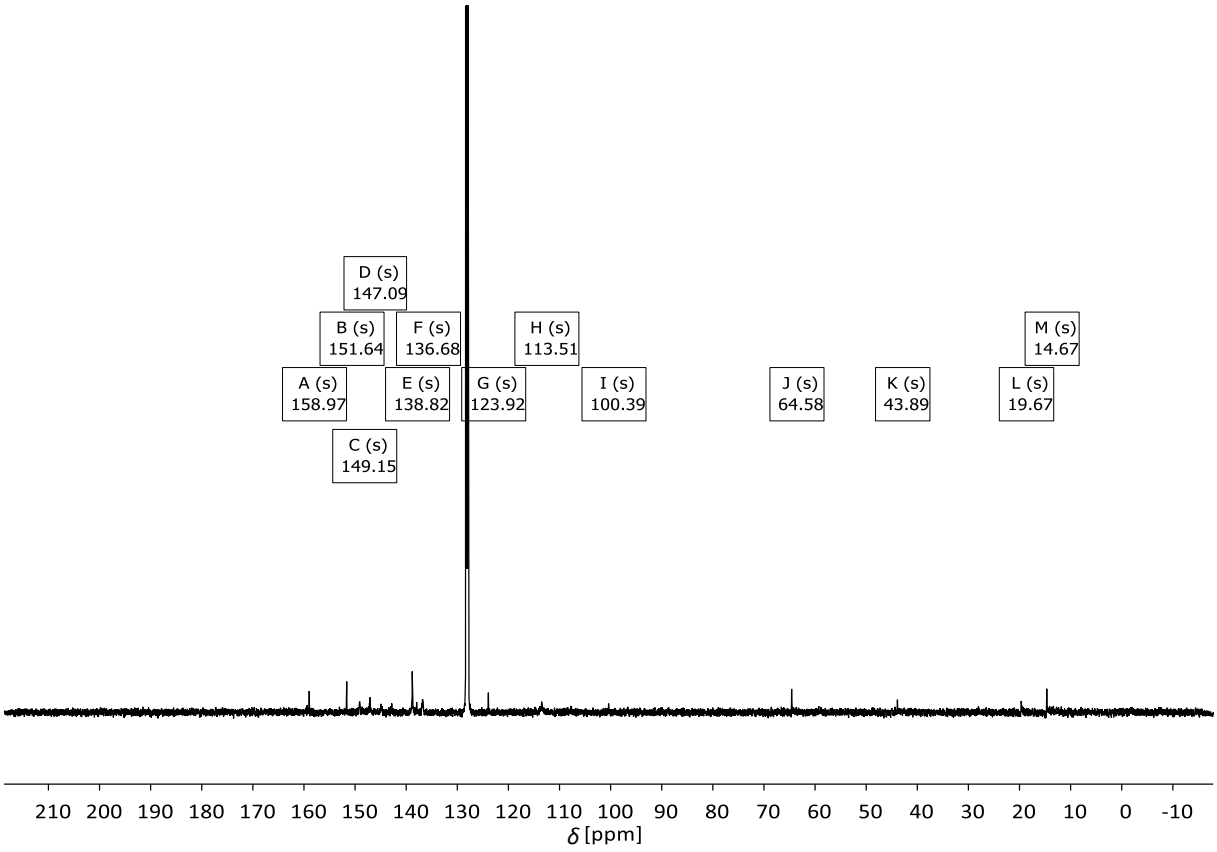

Figure S12 ^{13}C{^{1}H} NMR spectrum of a solution of 2,3,6,7,10,11-hexakis(bis(pentafluorophenyl)boryl)vinyl-4b,8b,12b-tri-*n*-propyltribenzotriquinacene (**6**) in C_6D_6 (160 MHz, 293 K).

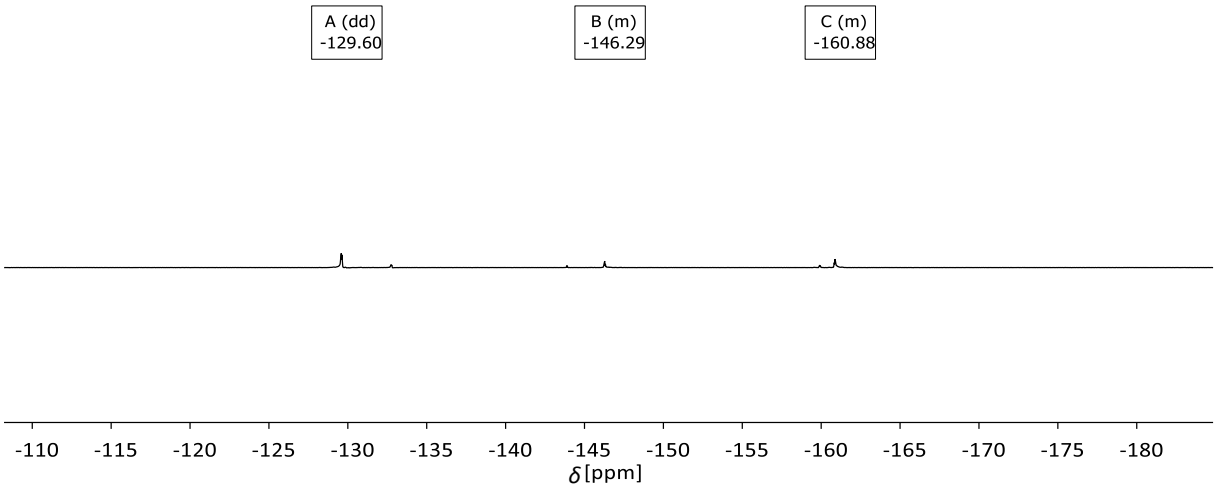

Figure S13 ^{19}F NMR spectrum of a solution of 2,3,6,7,10,11-hexakis(bis(pentafluorophenyl)boryl)vinyl-4b,8b,12b-tri-*n*-propyl-tribenzotriquinacene (**6**) in C_6D_6 (126 MHz, 293 K).

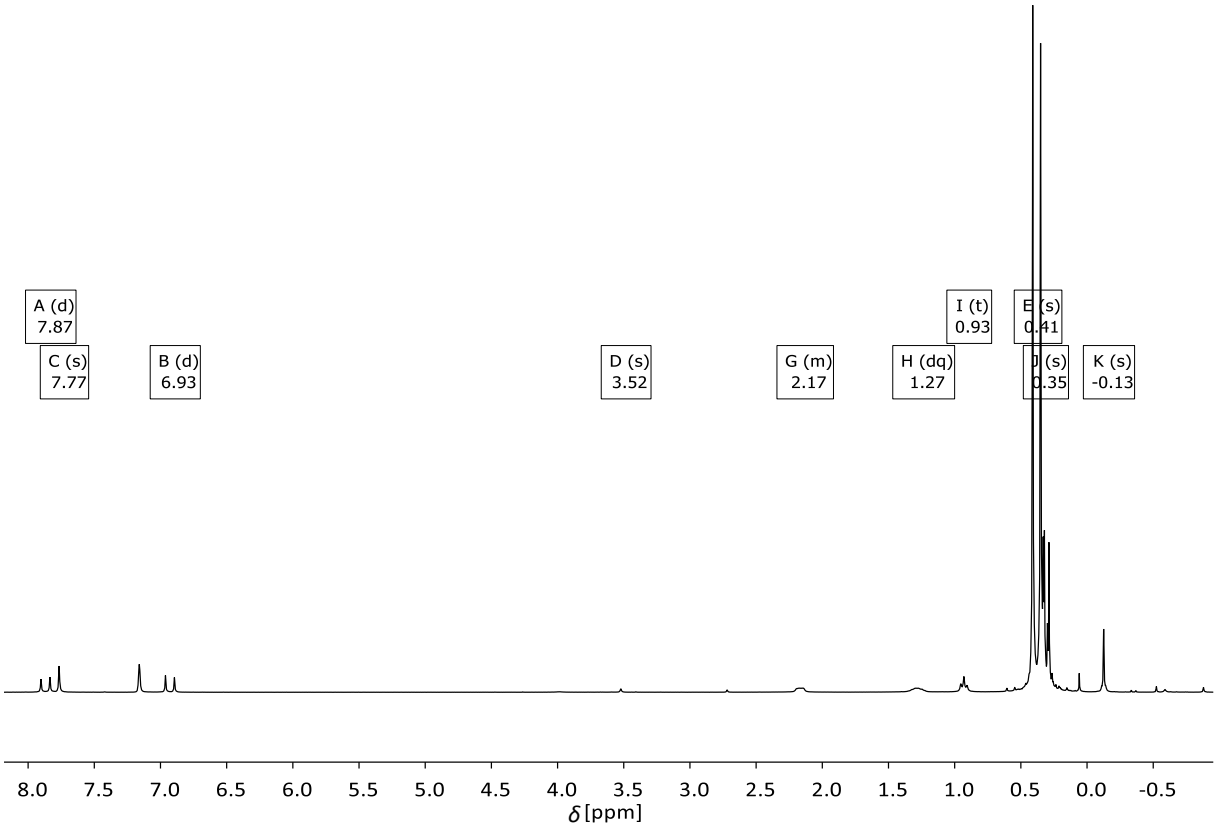

Figure S14 ^{1}H NMR spectrum of a solution of 2,3,6,7,10,11-hexakis(2-bis(bis(trimethylsilylmethyl)aluminyl)vinyl-4b,8b,12b-tri-*n*-propyltribenzotriquinacene (**7**) in C_6D_6 (500 MHz, 293 K).

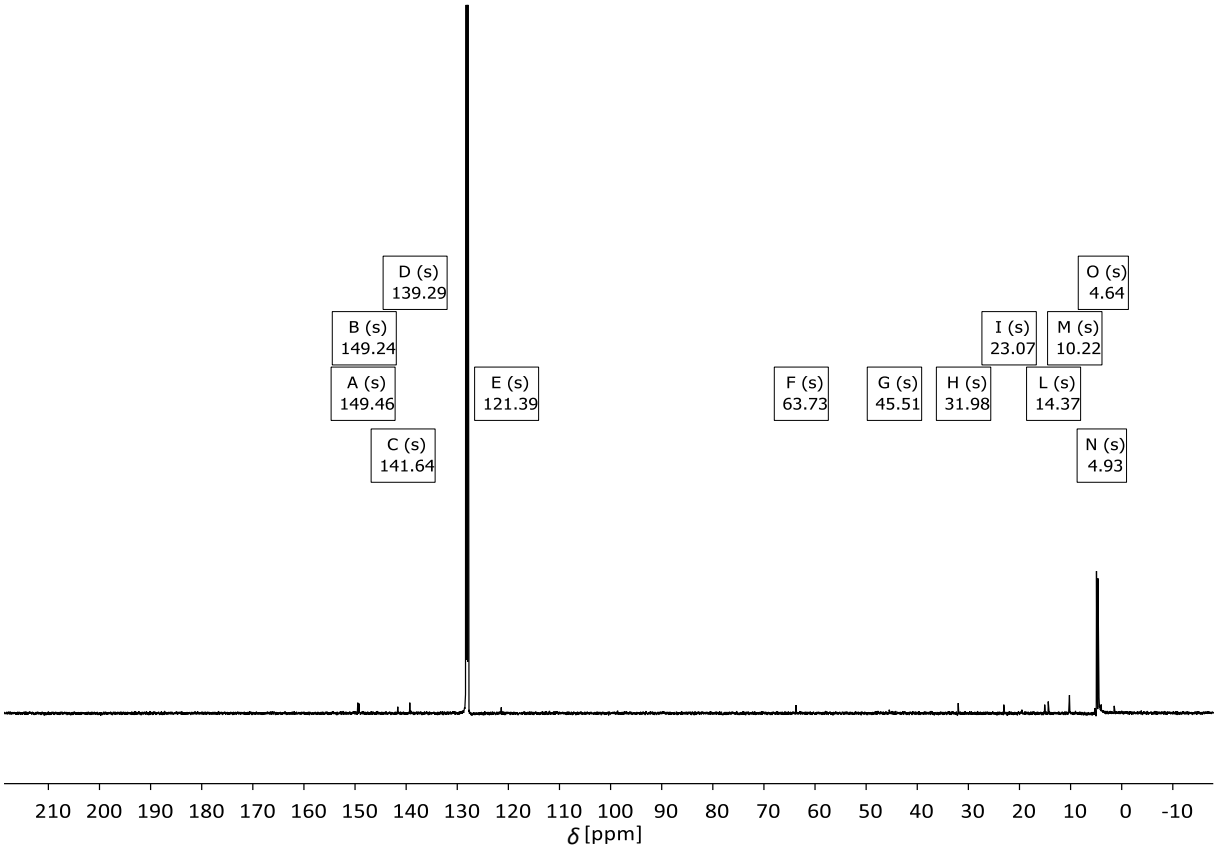

Figure S15 $^{13}C\{^{1}H\}$ NMR spectrum of a solution of 2,3,6,7,10,11-hexakis(2-bis(bis(trimethylsilylmethyl)aluminyl)vinyl-4b,8b,12b-tri-*n*-propyltribenzotriquinacene (**7**) in C_6D_6 (126 MHz, 293 K).

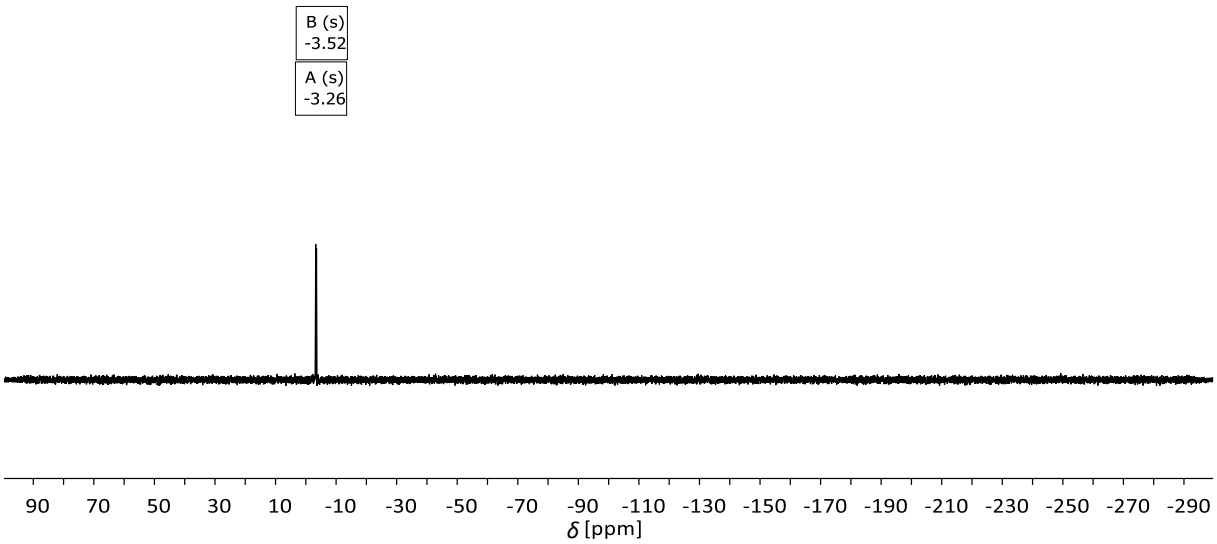

Figure S16 $^{29}Si\{^{1}H\}$ NMR spectrum of a solution of 2,3,6,7,10,11-hexakis(2-bis(bis(trimethylsilylmethyl)aluminyl)vinyl-4b,8b,12b-tri-*n*-propyltribenzotriquinacene (**7**) in C_6D_6 (99 MHz, 293 K).

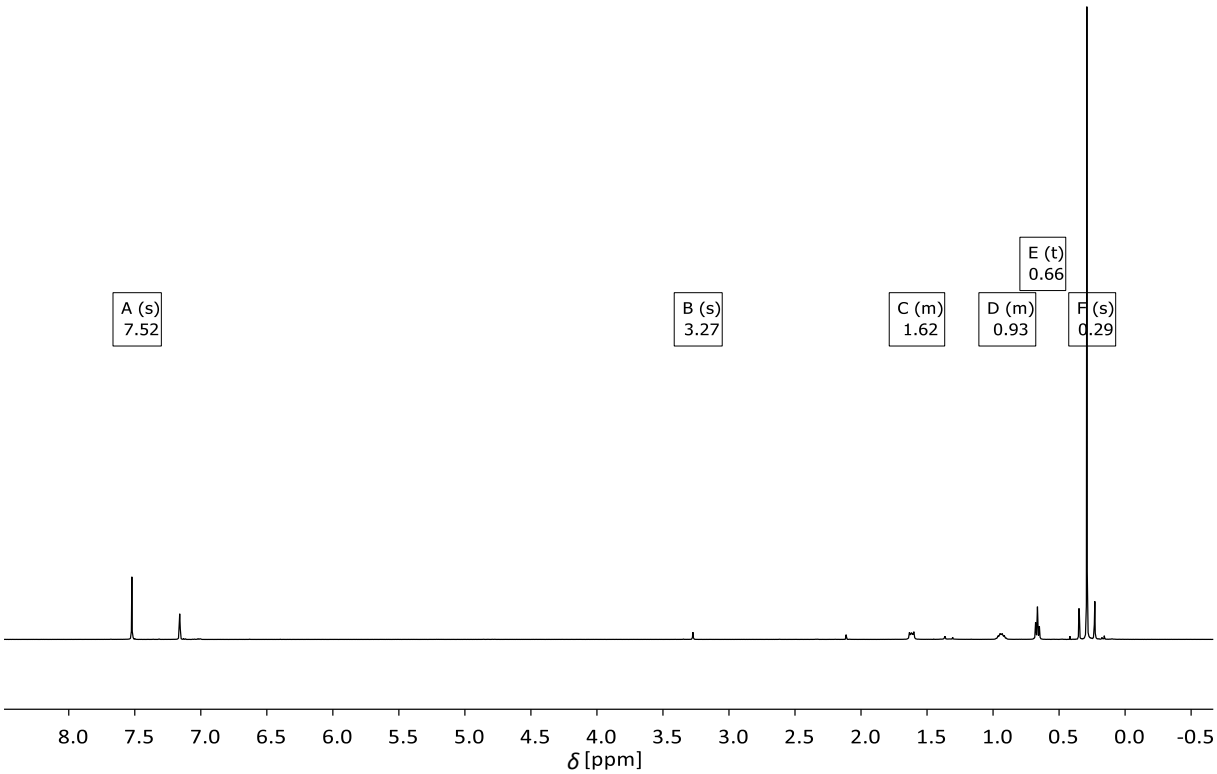

Figure S17 ^{1}H NMR spectrum of a solution of 2,3,6,7,10,11-hexakis((trimethylstannyl)ethynyl)- 4b,8b,12b-tri-*n*-propyltribenzotriquinacene (**8**) in C_6D_6 (500 MHz, 293 K).

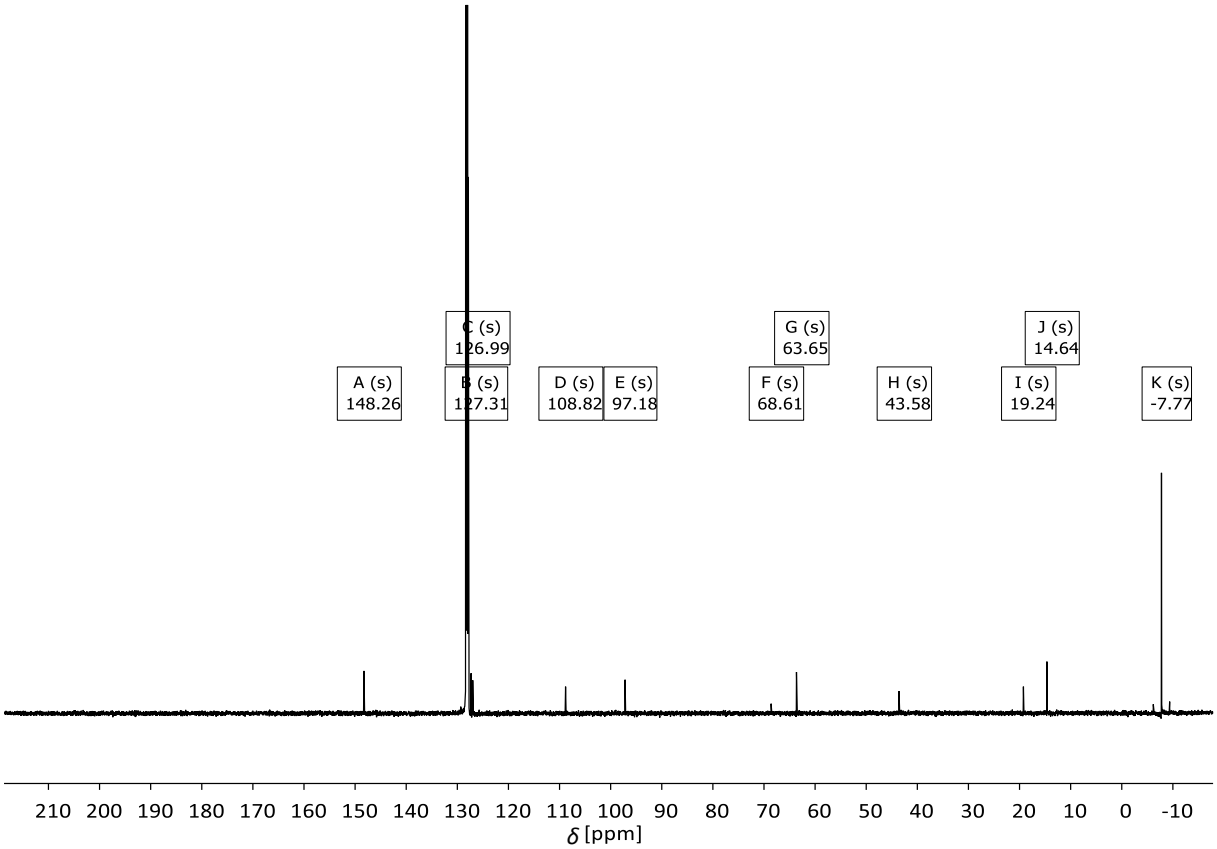

Figure S18 $^{13}C\{^{1}H\}$ NMR spectrum of a solution of 2,3,6,7,10,11-hexakis((trimethylstannyl)ethynyl)- 4b,8b,12b-tri-*n*-propyltribenzotriquinacene (**8**) in C_6D_6 (126 MHz, 293 K).

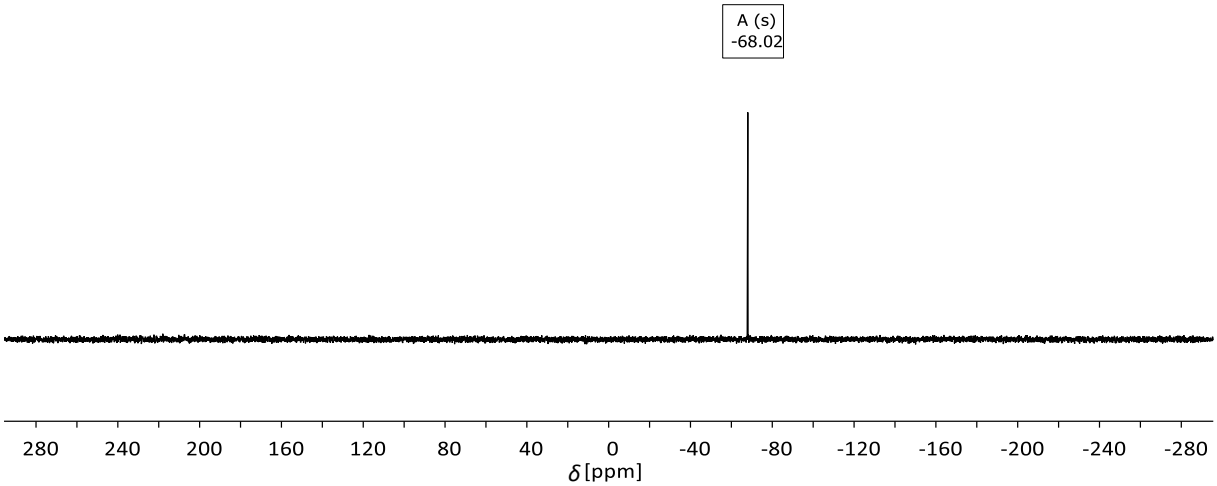

Figure S19 $^{119}Sn\{^{1}H\}$ NMR spectrum of a solution of 2,3,6,7,10,11-hexakis((trimethylstannyl)ethynyl)- 4b,8b,12b-tri-*n*-propyltribenzotriquinacene (**8**) in C_6D_6 (187 MHz, 293 K).

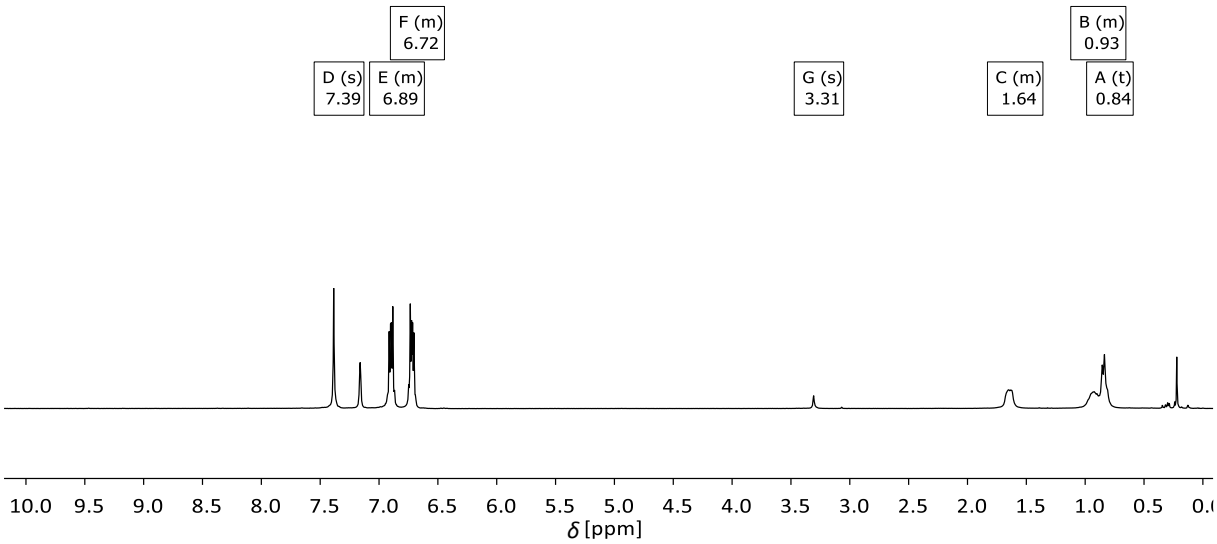

Figure S20 ^{1}H NMR spectrum of a solution of 2,3,6,7,10,11-hexakis((benzo[*d*][1,3,2]dioxaborol-2-yl)ethynyl)- 4b,8b,12b-tri-*n*-propyltribenzotriquinacene (**9**) in C_6D_6 (500 MHz, 293 K).

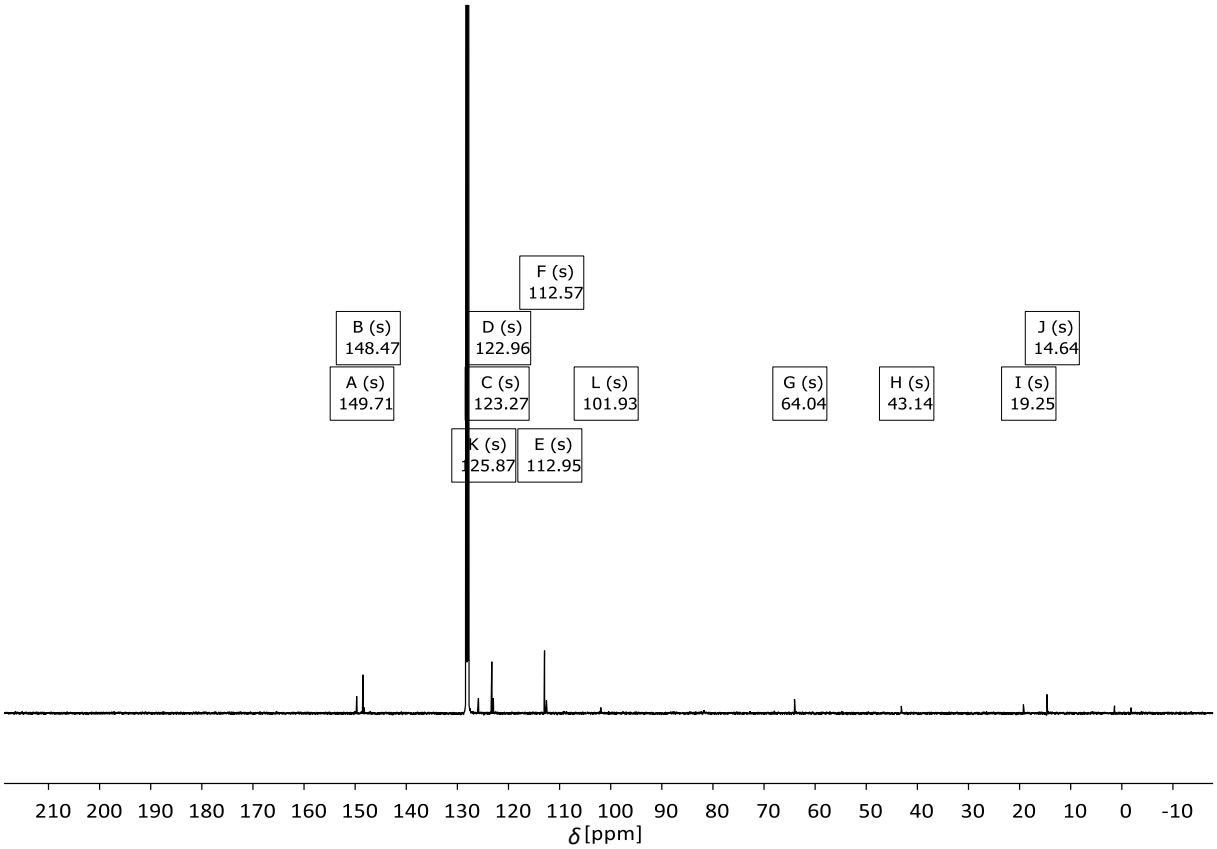

Figure S21 $^{13}C\{^{1}H\}$ NMR spectrum of a solution of 2,3,6,7,10,11-hexakis((benzo[*d*][1,3,2]dioxaborol-2-yl)ethynyl)-4b,8b,12b-tri-*n*-propyltribenzotriquinacene (**9**) in C_6D_6 (126 MHz, 293 K).

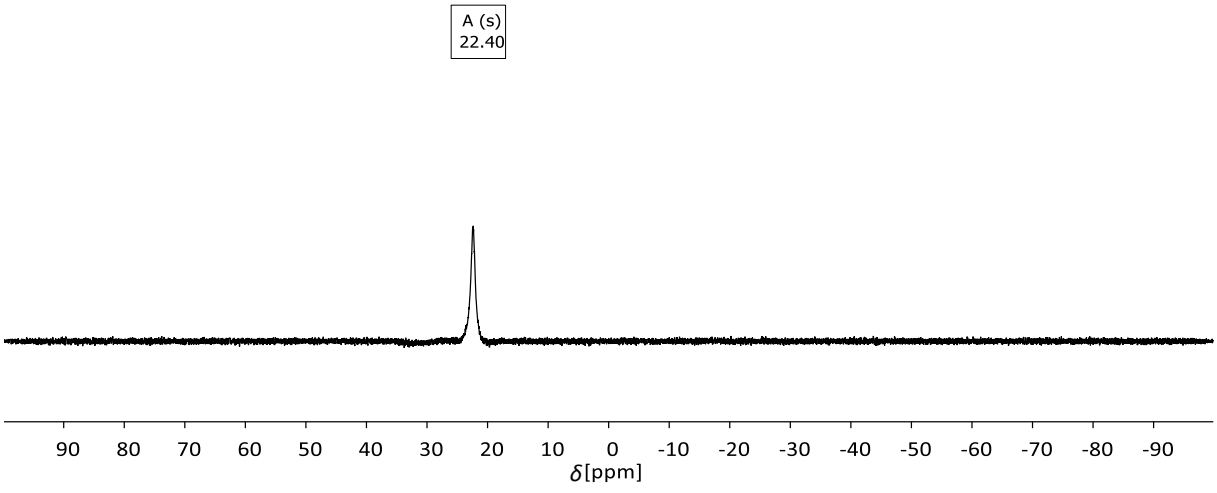

Figure S22 ^{11}B NMR spectrum of a solution of 2,3,6,7,10,11-hexakis((benzo[*d*][1,3,2]dioxaborol-2-yl)ethynyl)- 4b,8b,12b-tri-*n*-propyltribenzotriquinacene (**9**) in C_6D_6 (160 MHz, 293 K).

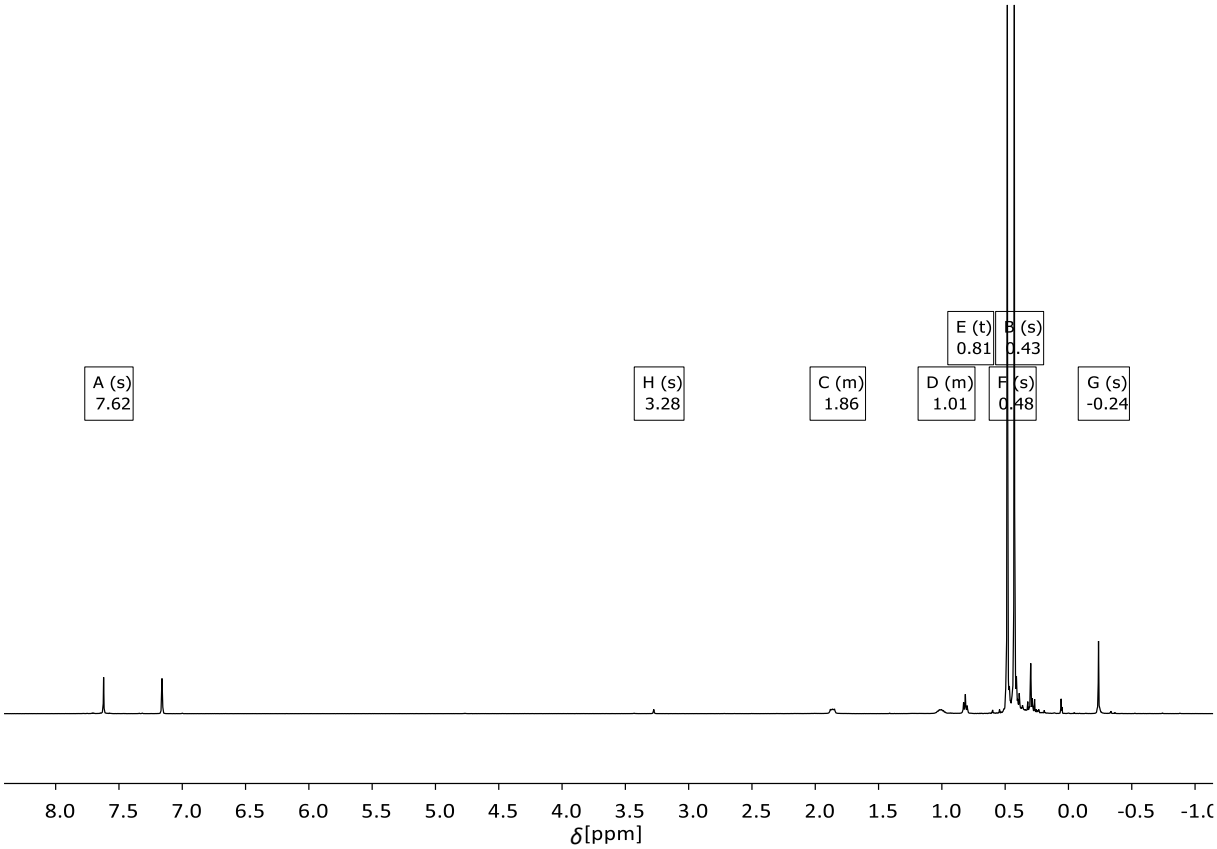

Figure S23 ^{1}H NMR spectrum of a solution of 2,3,6,7,10,11-hexakis(2-bis(bis(trimethylsilylmethyl)aluminyl)ethynyl)-4b,8b,12b-tri-*n*-propyltribenzotriquinacene (**10**) in C_6D_6 (500 MHz, 293 K).

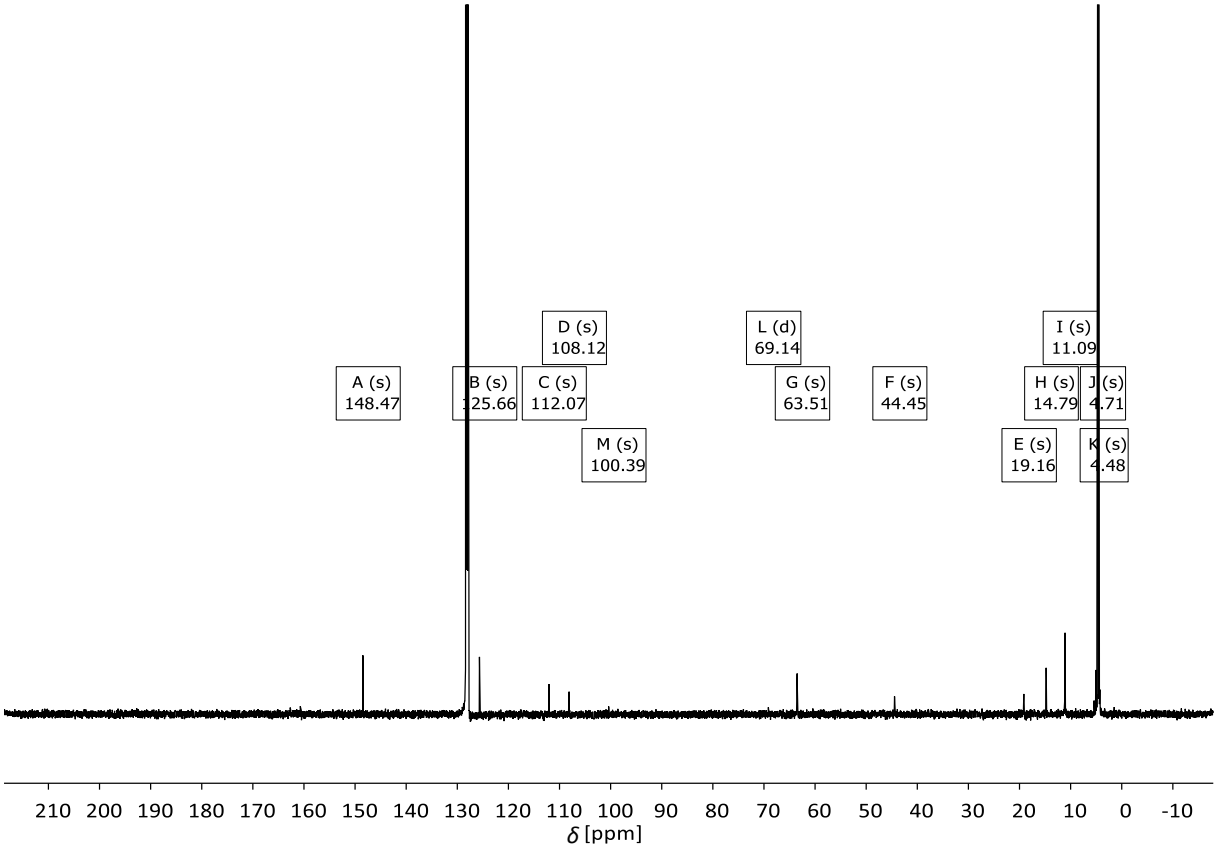

Figure S24 ^{13}C{^{1}H} NMR spectrum of a solution of 2,3,6,7,10,11-hexakis(2-bis(bis(trimethylsilylmethyl)aluminyl)ethynyl)-4b,8b,12b-tri-*n*-propyltribenzotriquinacene (**10**) in C_6D_6 (126 MHz, 293 K).

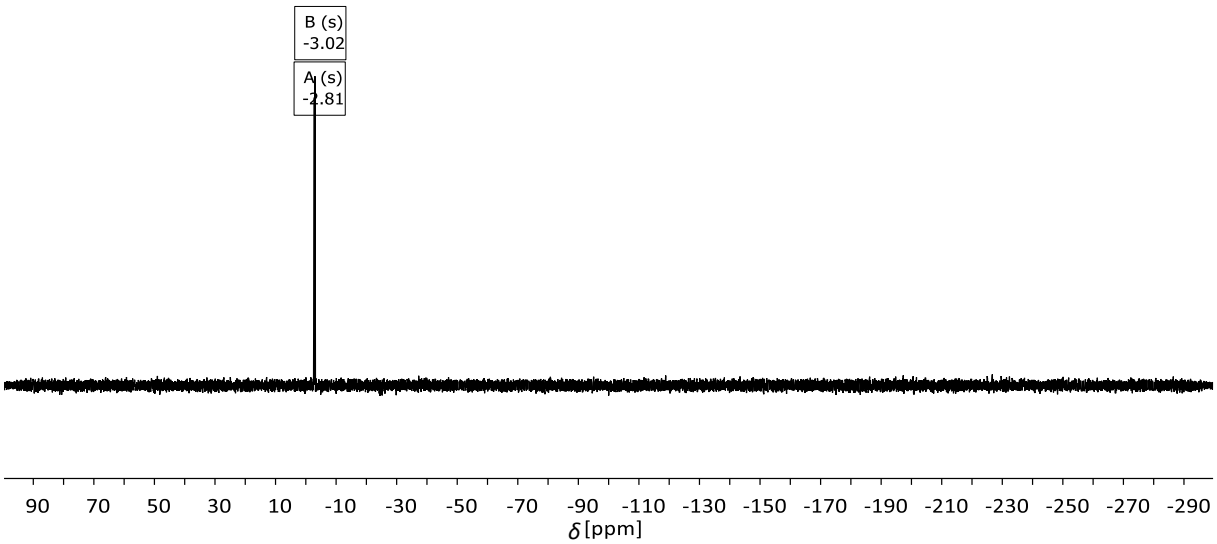

Figure S25 $^{29}Si\{^{1}H\}$ NMR spectrum of a solution of 2,3,6,7,10,11-hexakis(2-bis(bis(trimethylsilylmethyl)aluminyl)ethynyl)-4b,8b,12b-tri-*n*-propyltribenzotriquinacene (**10**) in C_6D_6 (99 MHz, 293 K).

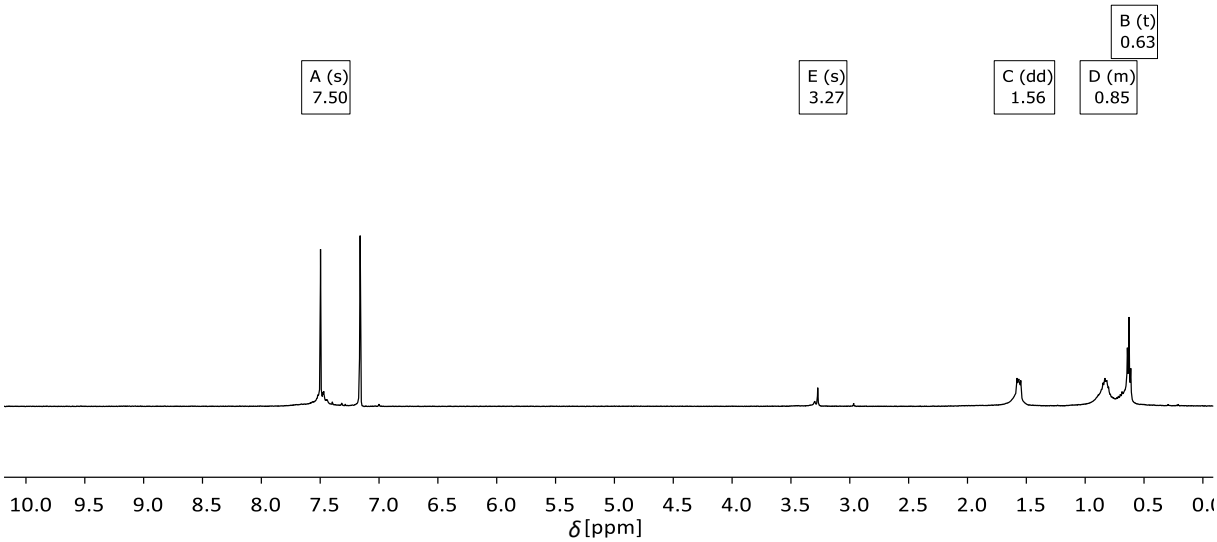

Figure S26 ^{1}H NMR spectrum of a solution of 2,3,6,7,10,11-hexakis((pentafluroethyl)stibanyl)ethynyl)- 4b,8b,12b-tri-*n*-propyltribenzotriquinacene (**11**) in C_6D_6 (500 MHz, 293 K).

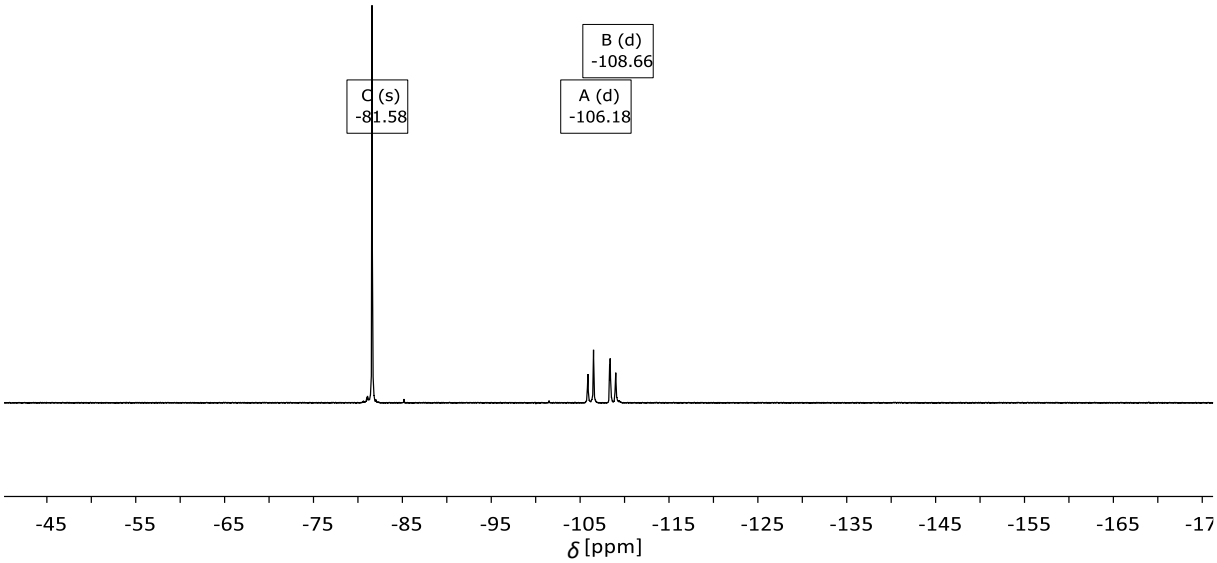

Figure S27 ^{19}F NMR spectrum of a solution of 2,3,6,7,10,11-hexakis((pentafluroethyl)stibanyl)ethynyl)- 4b,8b,12b-tri-*n*-propyltribenzotriquinacene (**11**) in C_6D_6 (126 MHz, 293 K).

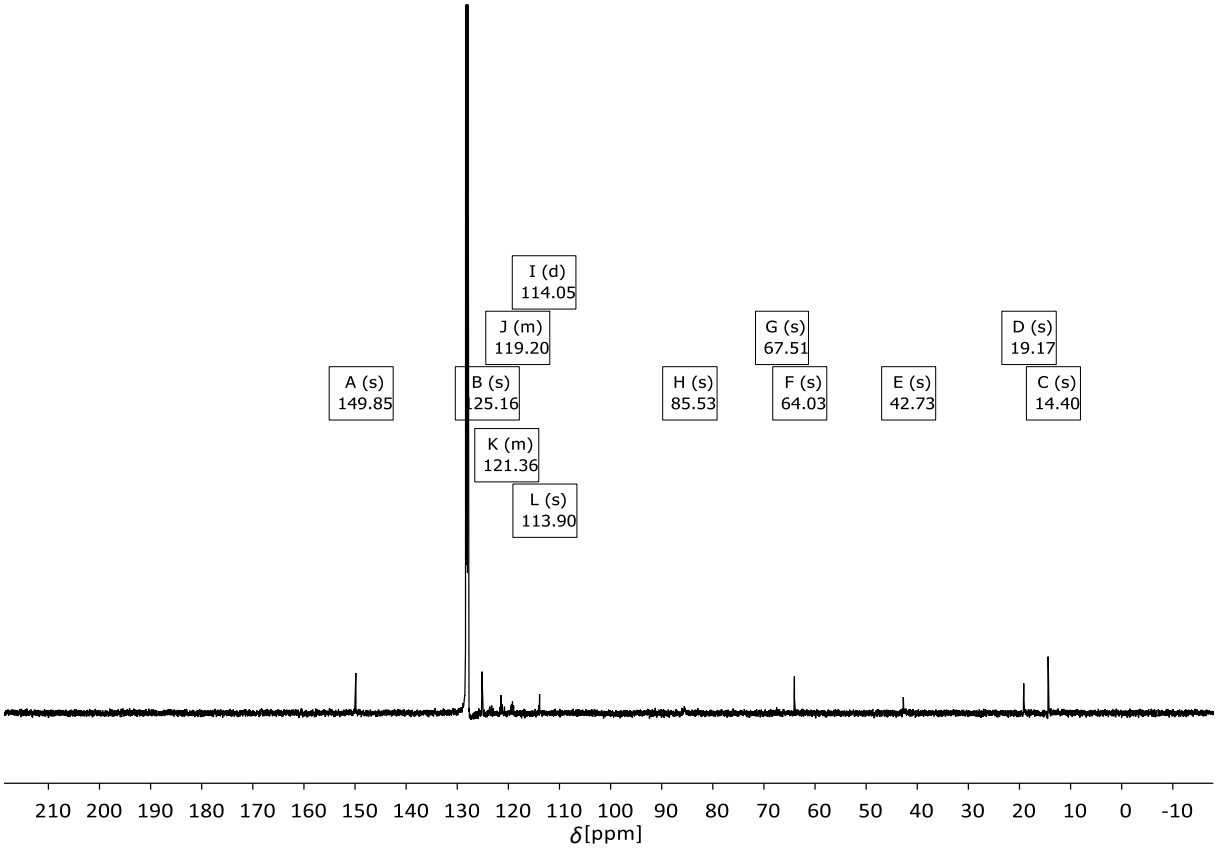

Figure S28 $^{13}C\{^1H\}$ NMR spectrum of a solution of 2,3,6,7,10,11-hexakis((pentafluroethyl)stibanyl)ethynyl)- 4b,8b,12b-tri-*n*-propyltribenzotriquinacene (**11**) in C_6D_6 (126 MHz, 293 K).

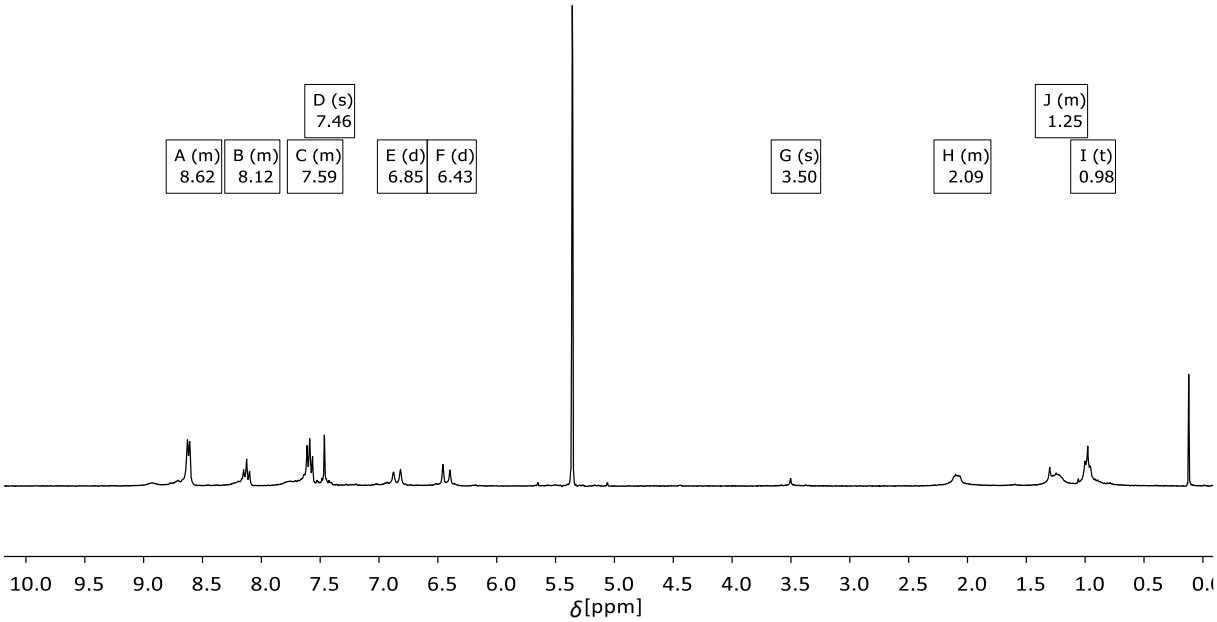

Figure S29 ^{1}H NMR spectrum of a solution of 2,3,6,7,10,11-hexakis(bis(pentafluorophenyl)boryl)vinyl-4b,8b,12b-tri-*n*-propyltribenzotriquinacene (**6**)·6 pyridine in CD_2Cl_2 (500 MHz, 293 K).

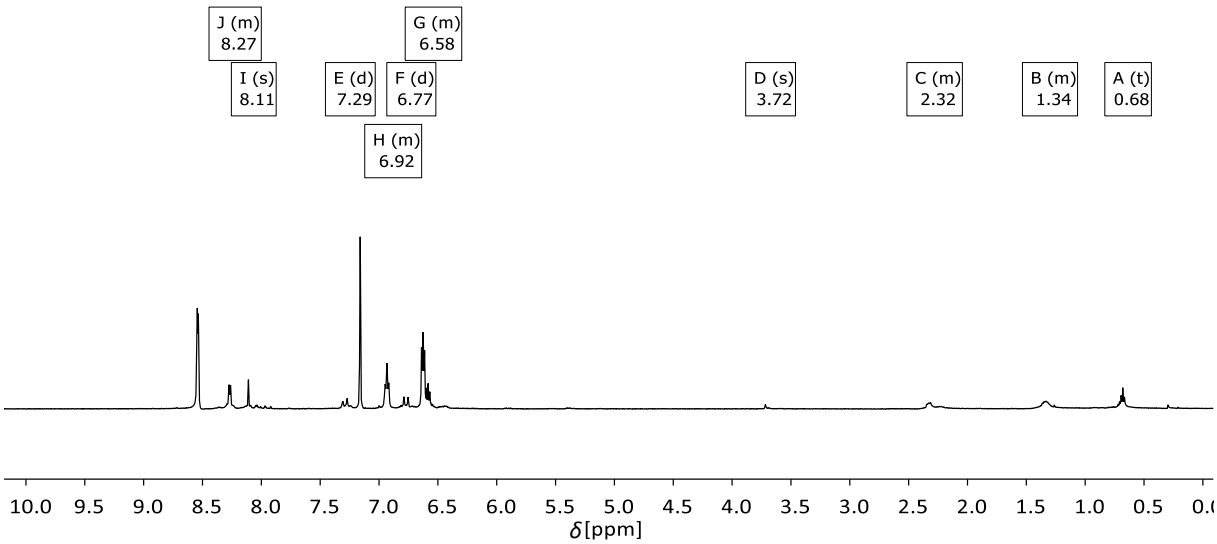

Figure S30 ^{1}H NMR spectrum of a solution of 2,3,6,7,10,11-hexakis(bis(pentafluorophenyl)boryl)vinyl-4b,8b,12b-tri-*n*-propyltribenzotriquinacene (**6**)·6 pyridine in C_6D_6 (500 MHz, 293 K).

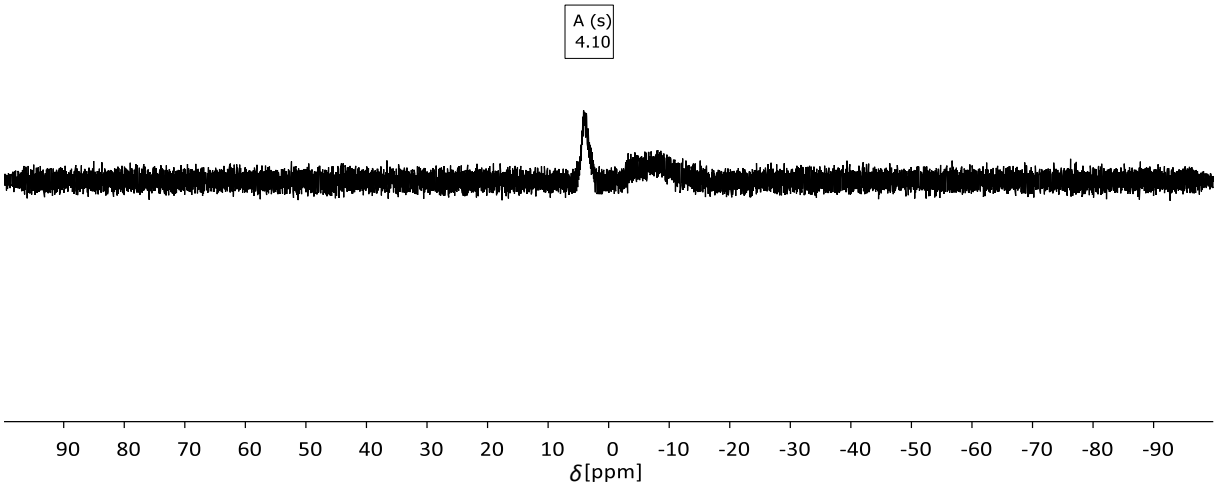

Figure S31 ^{11}B NMR spectrum of a solution of 2,3,6,7,10,11-hexakis(bis(pentafluorophenyl)boryl)vinyl-4b,8b,12b-tri-*n*-propyltribenzotriquinacene (**6**)·6 pyridine in C_6D_6 (160 MHz, 293 K).

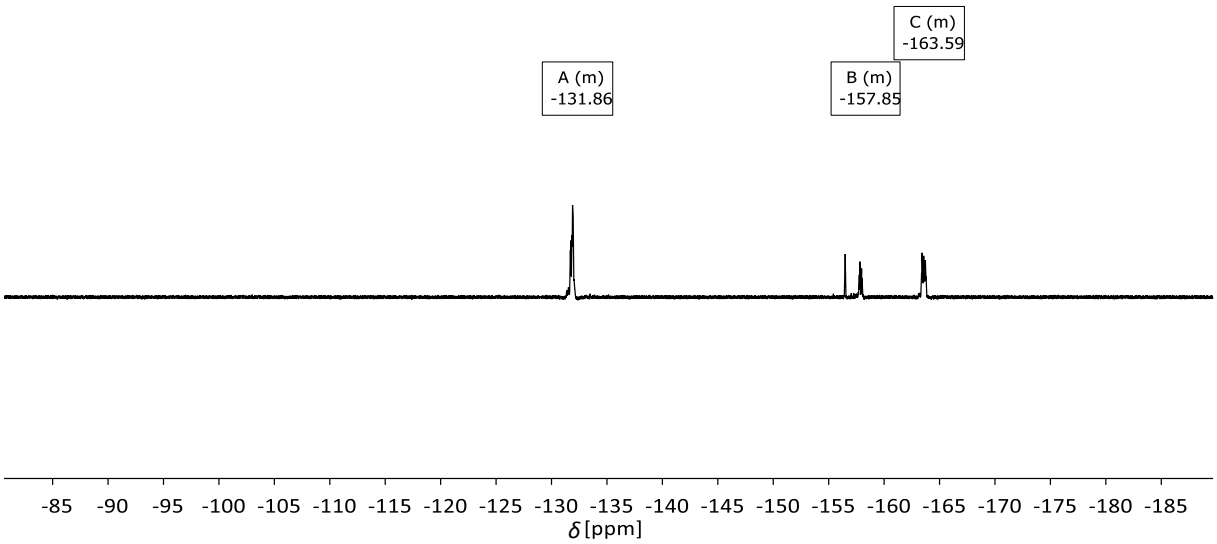

Figure S32 ^{19}F NMR spectrum of a solution of 2,3,6,7,10,11-hexakis(bis(pentafluorophenyl)boryl)vinyl-4b,8b,12b-tri-*n*-propyltribenzotriquinacene (**6**)·6 pyridine in C_6D_6 (126 MHz, 293 K).

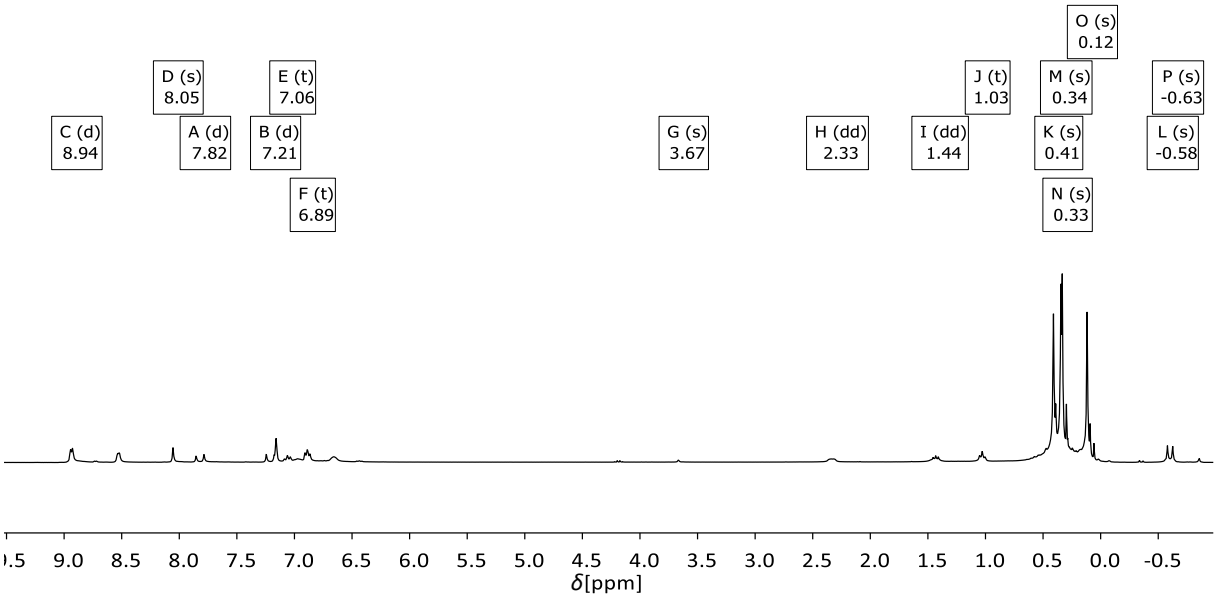

Figure S33 ^{1}H NMR spectrum of a solution of 2,3,6,7,10,11-hexakis(2-bis(bis(trimethylsilylmethyl)aluminyl)vinyl-4b,8b,12b-tri-*n*-propyltribenzotriquinacene (**7**)·6 pyridine in C_6D_6 (300 MHz, 293 K).

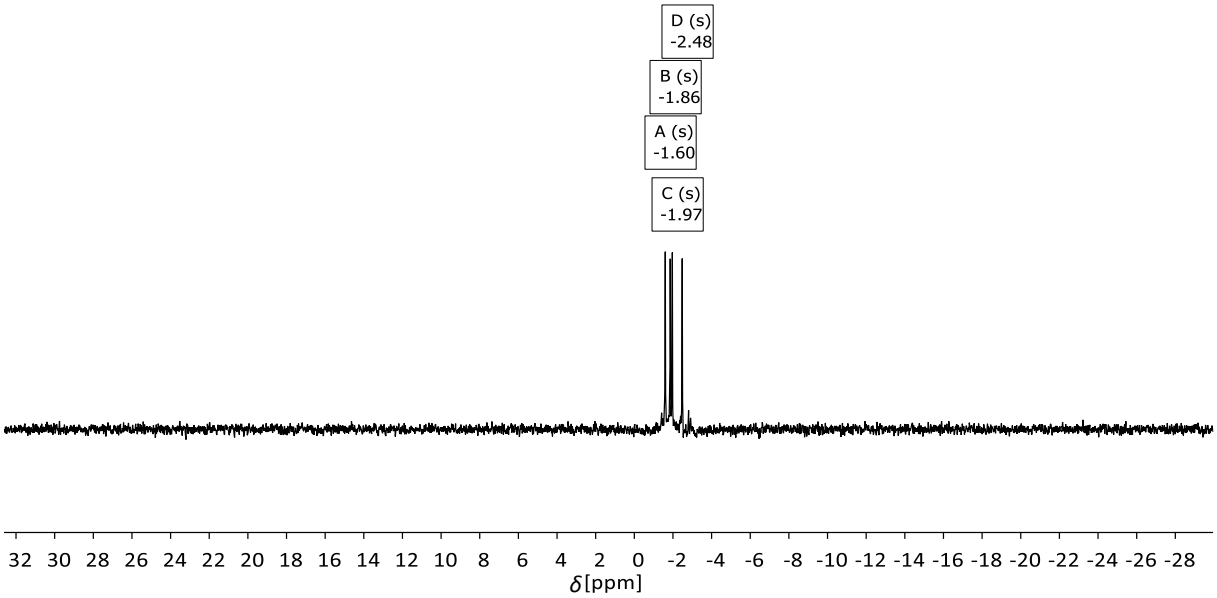

Figure S34 $^{29}Si\{^{1}H\}$ NMR spectrum of a solution of 2,3,6,7,10,11-hexakis(2-bis(bis(trimethylsilylmethyl)aluminyl)vinyl-4b,8b,12b-tri-*n*-propyltribenzotriquinacene (**7**)·6 pyridine in C_6D_6 (99 MHz, 293 K).

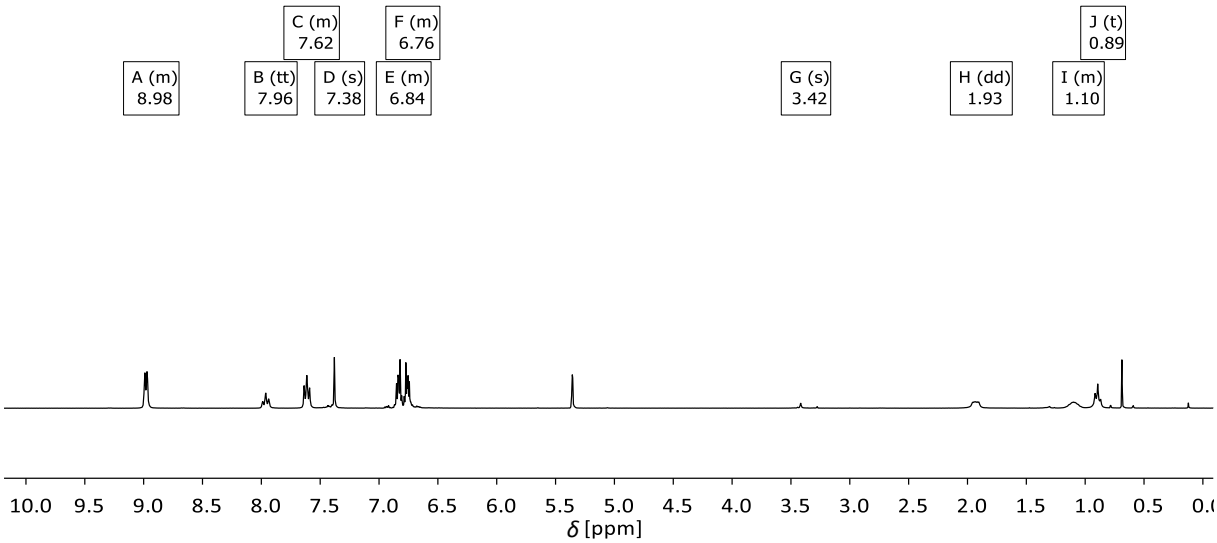

Figure S35 ^{1}H NMR spectrum of a solution of 2,3,6,7,10,11-hexakis((benzo[*d*][1,3,2]dioxaborol-2-yl)ethynyl)-4b,8b,12b-tri-*n*-propyltribenzotriquinacene (**9**)·6 pyridine in CD_2Cl_2 (500 MHz, 293 K).

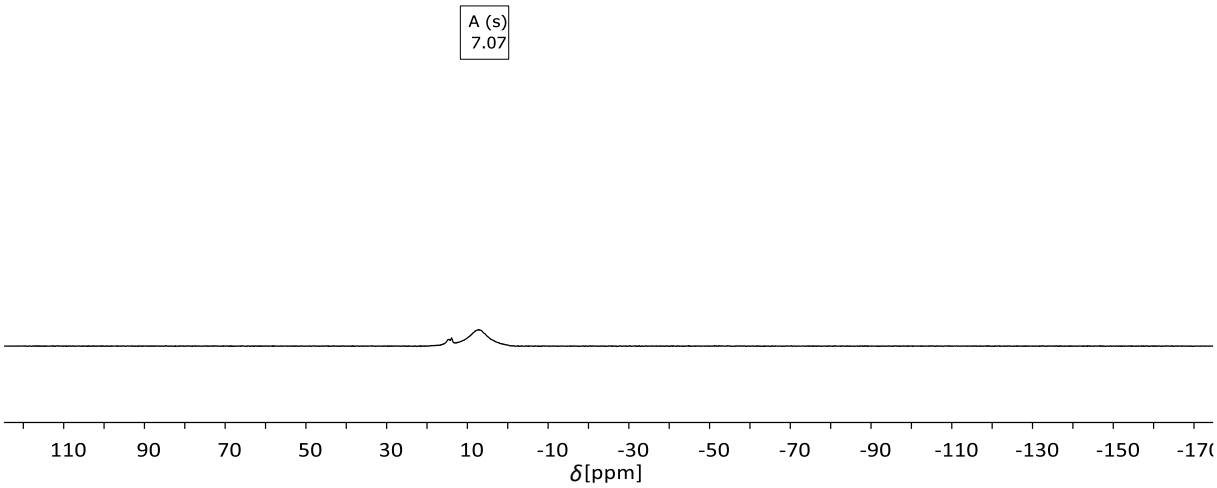

Figure S36 ^{11}B NMR spectrum of a solution of 2,3,6,7,10,11-hexakis((benzo[*d*][1,3,2]dioxaborol-2-yl)ethynyl)-4b,8b,12b-tri-*n*-propyltribenzotriquinacene (**9**)·6 pyridine in CD_2Cl_2 (160 MHz, 293 K).

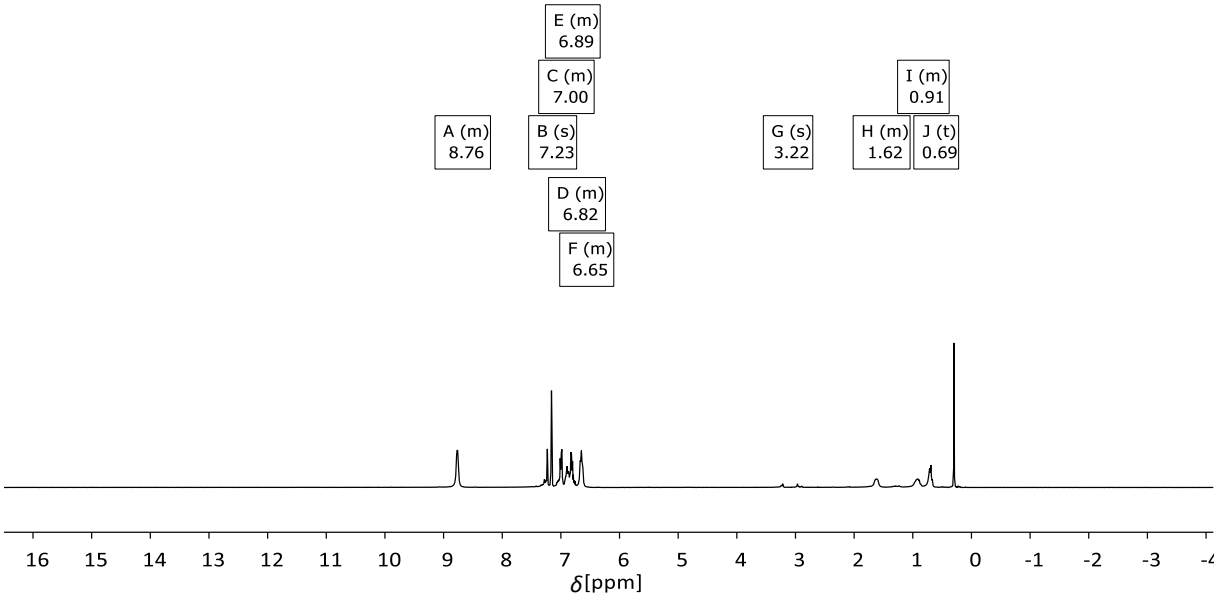

Figure S37 ^{1}H NMR spectrum of a solution of 2,3,6,7,10,11-Hexakis((benzo[*d*][1,3,2]dioxaborol-2-yl)ethynyl)-4b,8b,12b-tri-*n*-propyltribenzotriquinacene (**9**)·6 pyridine in C_6D_6 (300 MHz, 293 K).

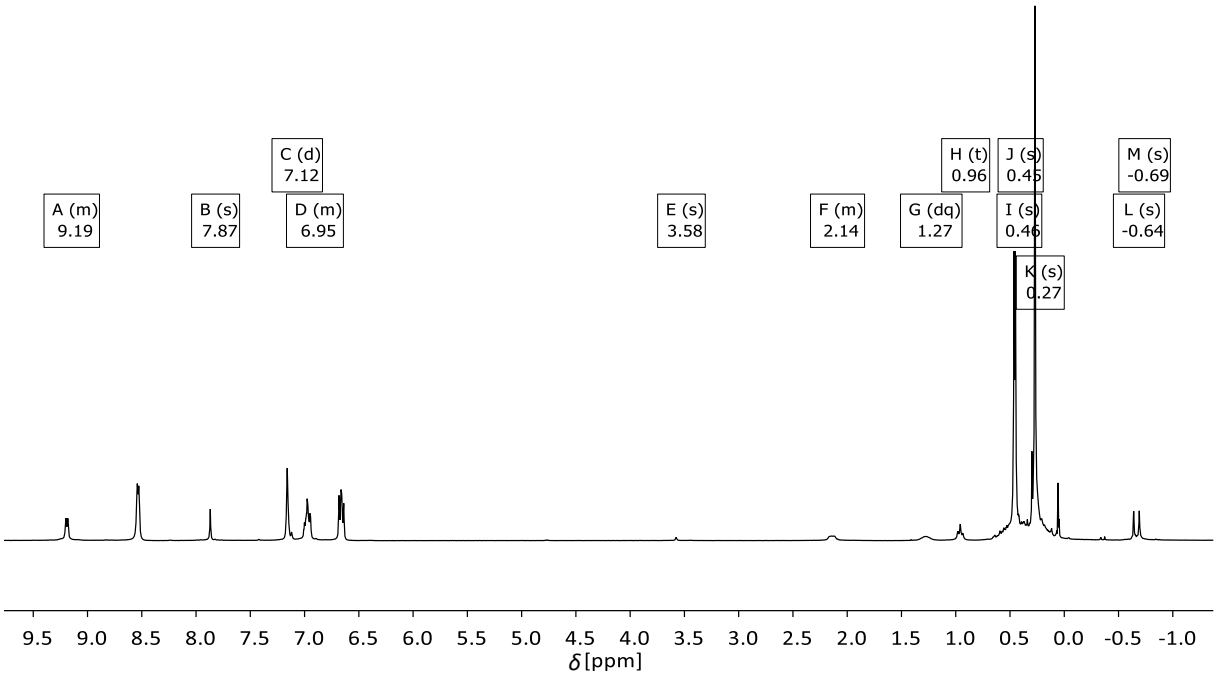

Figure S38 ^{1}H NMR spectrum of a solution of 2,3,6,7,10,11-hexakis(2-bis(bis(trimethylsilylmethyl)aluminyl)ethynyl)-4b,8b,12b-tri-*n*-propyltribenzotriquinacene (**10**)·6 pyridine in C_6D_6 (500 MHz, 293 K).

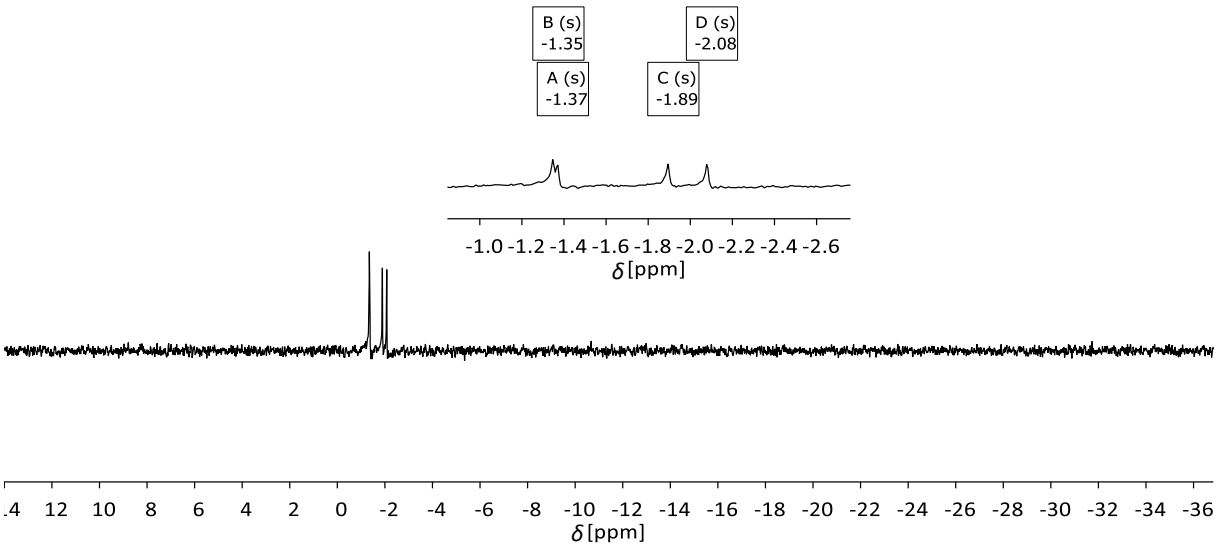

Figure S39 ^{29}Si{^{1}H} NMR spectrum of a solution of 2,3,6,7,10,11-hexakis(2-bis(bis(trimethylsilylmethyl)aluminyl)ethynyl)-4b,8b,12b-tri-*n*-propyltribenzotriquinacene (**10**)·6 pyridine in C_6D_6 (500 MHz, 293 K).

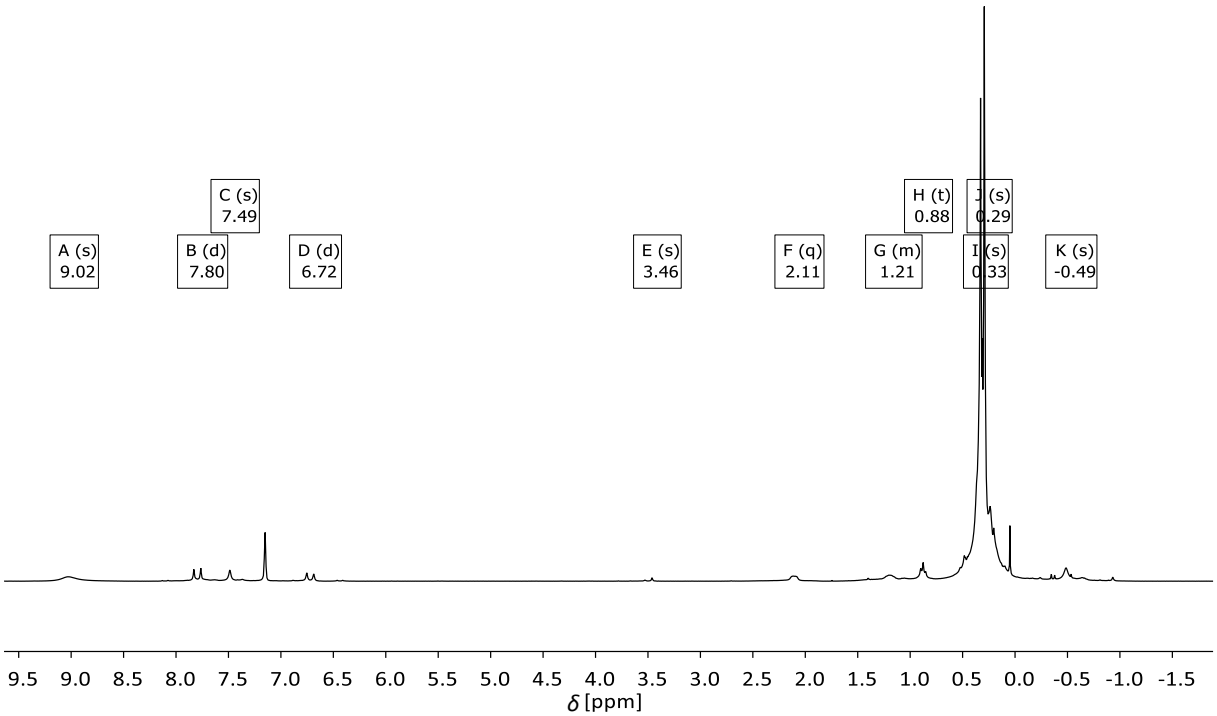

Figure S40 ^{1}H NMR spectrum of a solution of 2,3,6,7,10,11-hexakis(2-bis(bis(trimethylsilylmethyl)aluminyl)vinyl-4b,8b,12b-tri-*n*-propyltribenzotriquinacene (**7**)·3 pyrazine in C_6D_6 (500 MHz, 293 K).

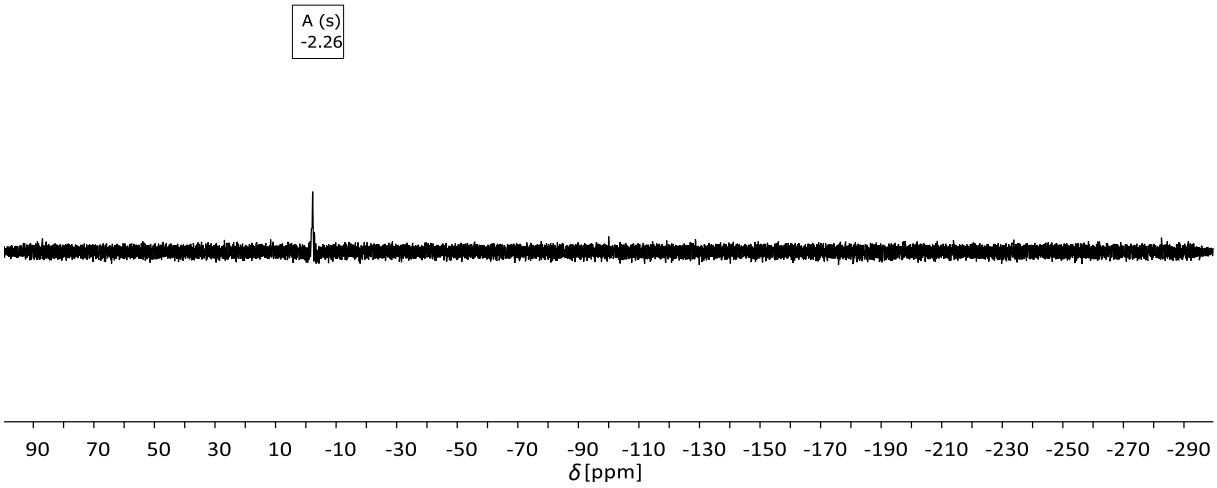

Figure S41 ^{29}Si{^{1}H} NMR spectrum of a solution of 2,3,6,7,10,11-hexakis(2-bis(bis(trimethylsilylmethyl)aluminyl)vinyl-4b,8b,12b-tri-*n*-propyltribenzotriquinacene (**7**)·3 pyrazine in C_6D_6 (99 MHz, 293 K).

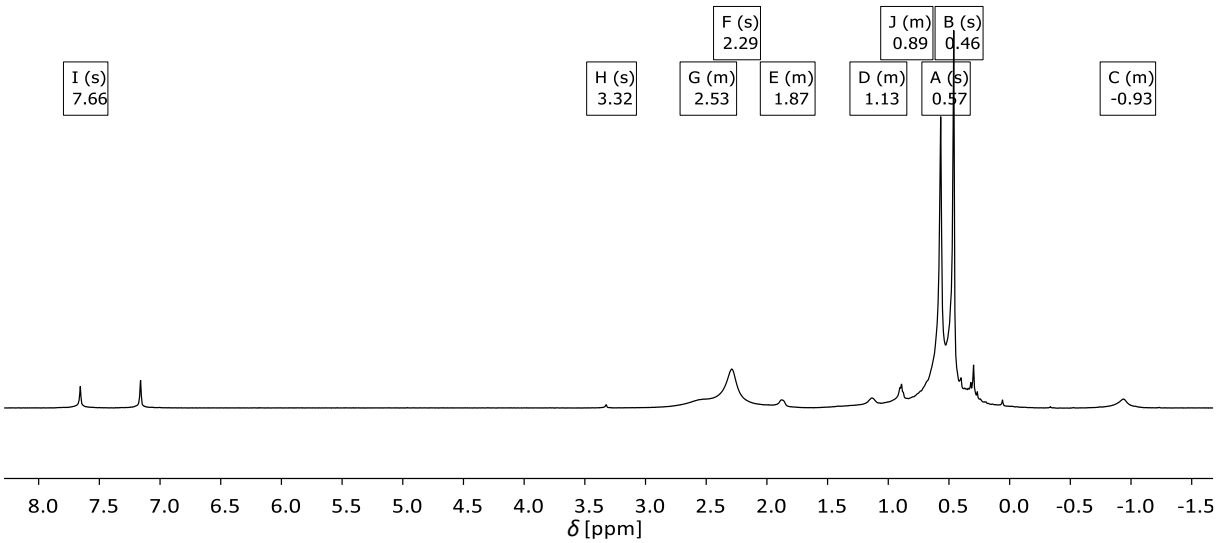

Figure S42 ^{1}H NMR spectrum of a solution of 2,3,6,7,10,11-hexakis(2-bis(bis(trimethylsilylmethyl)aluminyl)ethynyl-4b,8b,12b-tri-*n*-propyltribenzotriquinacene (**10**)·3 TMPDA in C_6D_6 (500 MHz, 293 K).

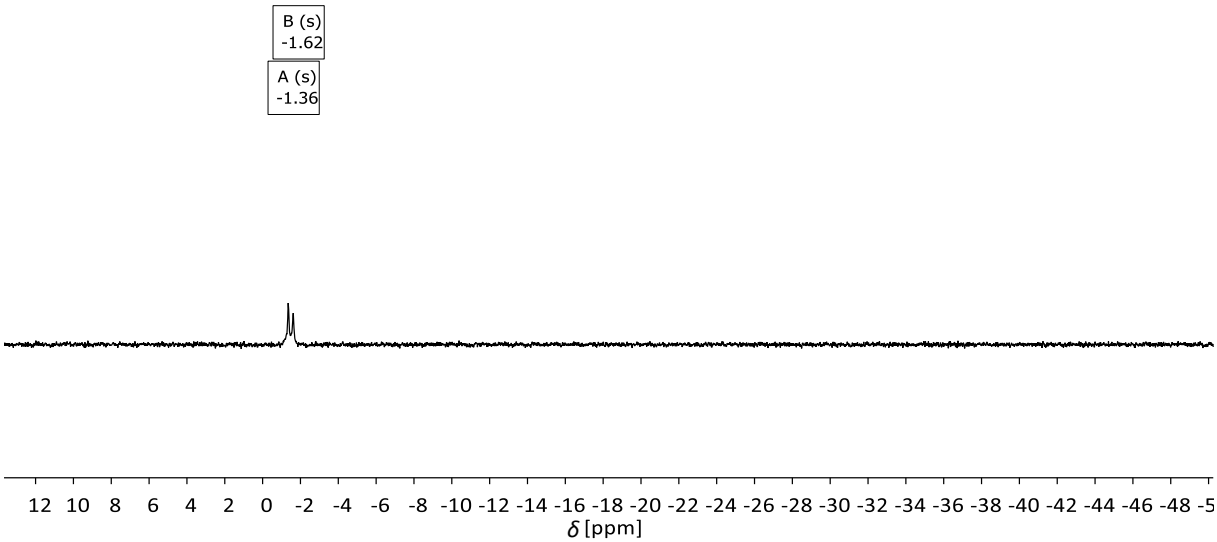

Figure S43 ^{29}Si{^{1}H} NMR spectrum of a solution of 2,3,6,7,10,11-hexakis(2-bis(bis(trimethylsilylmethyl)aluminyl)ethynyl-4b,8b,12b-tri-*n*-propyltribenzotriquinacene (**10**)·3 TMPDA in C_6D_6 (99 MHz, 293 K).

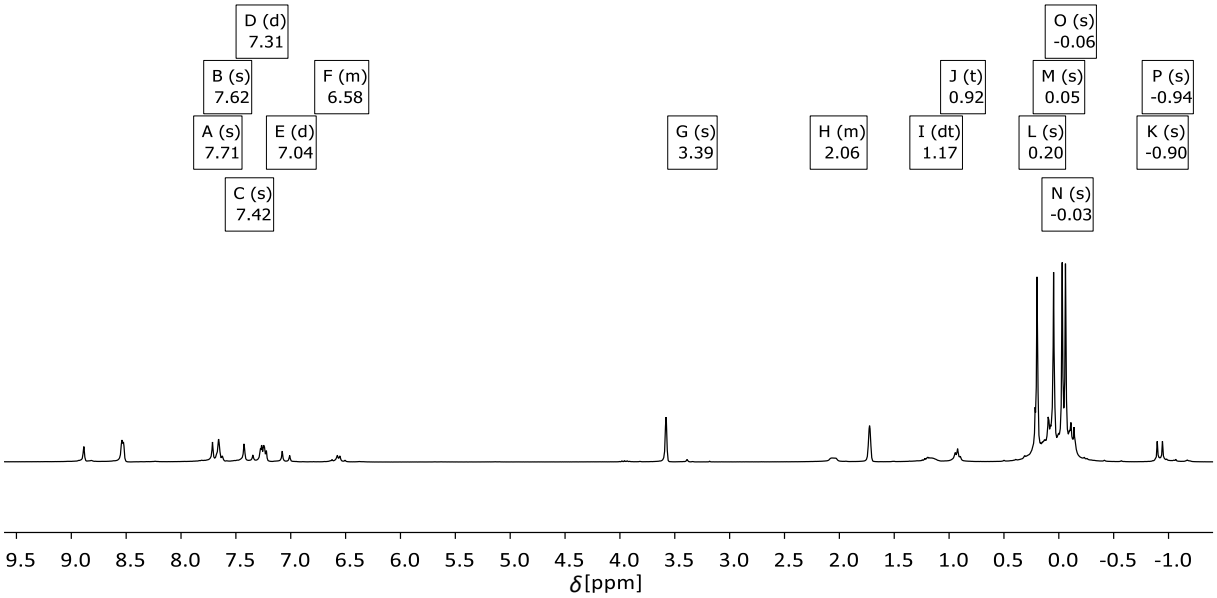

Figure S44 ^{1}H NMR spectrum of a solution of 2,3,6,7,10,11-hexakis(2-bis(bis(trimethylsilylmethyl)aluminyl)vinyl-4b,8b,12b-tri-*n*-propyltribenzotriquinacene (**7**)·3 BisImi in THF-*d*8 (500 MHz, 293 K).

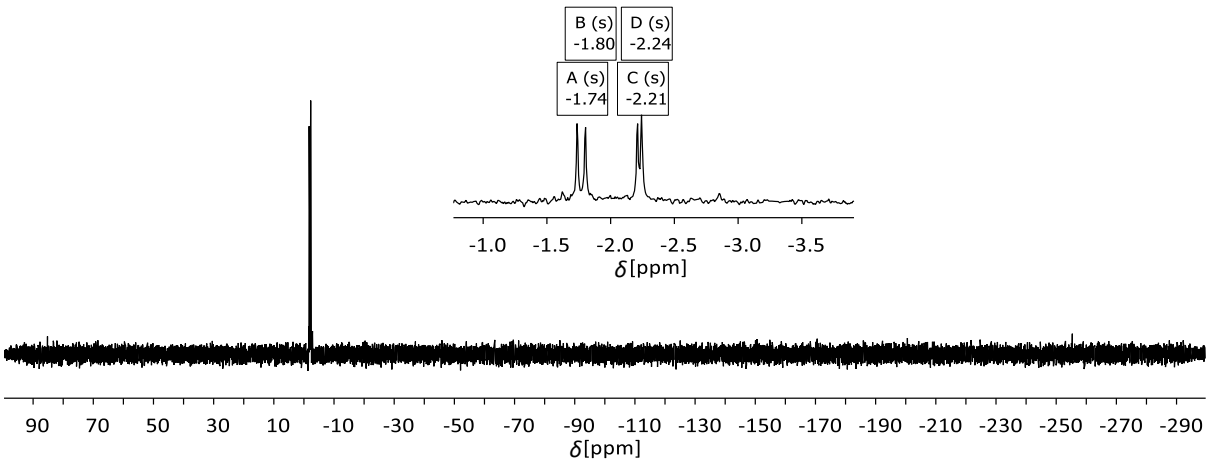

Figure S45 ^{29}Si{^{1}H} NMR spectrum of a solution of 2,3,6,7,10,11-hexakis(2-bis(bis(trimethylsilylmethyl)aluminyl)vinyl-4b,8b,12b-tri-*n*-propyltribenzotriquinacene (**7**)·3 BisImi in THF-*d*8 (99 MHz, 293 K).

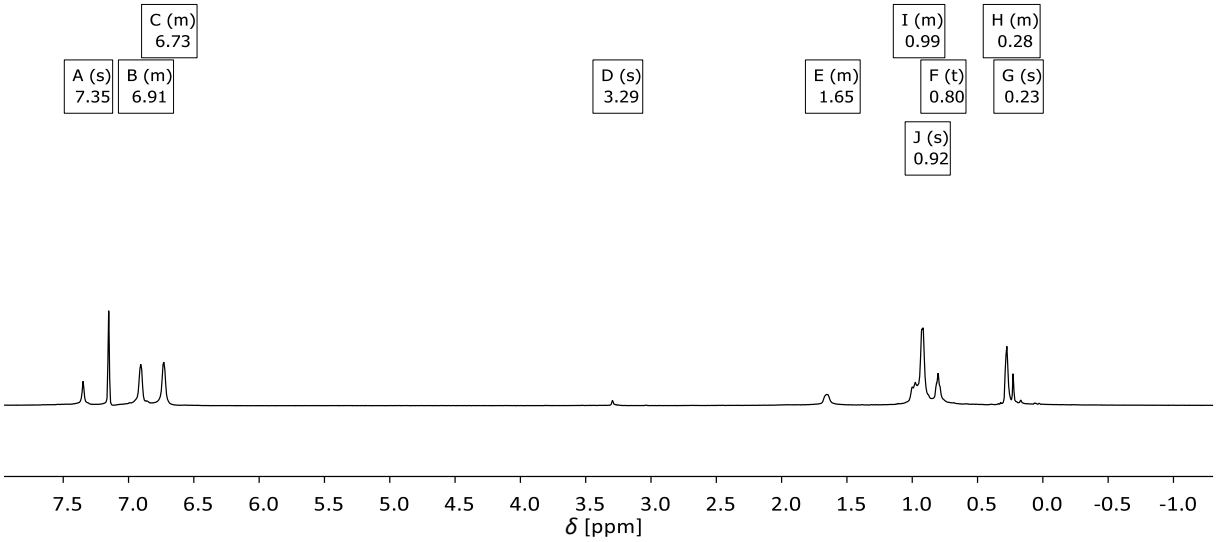

Figure S46 ^{1}H NMR spectrum of a solution of 2,3,6,7,10,11-hexakis((benzo[*d*][1,3,2]dioxaborol-2-yl)ethynyl)-4b,8b,12b-tri-*n*-propyltribenzotriquinacene (**9**)·3 BisPhos in C_6D_6 (500 MHz, 293 K).

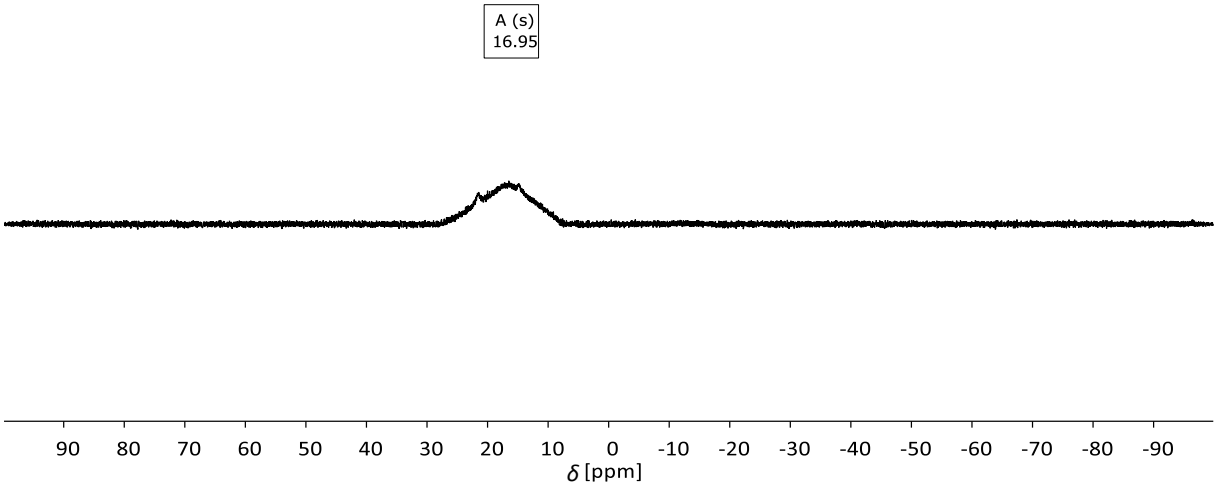

Figure S47 ^{11}B NMR spectrum of a solution of 2,3,6,7,10,11-hexakis((benzo[*d*][1,3,2]dioxaborol-2-yl)ethynyl)-4b,8b,12b-tri-*n*-propyltribenzotriquinacene (**9**)·3 BisPhos in C_6D_6 (160 MHz, 293 K).

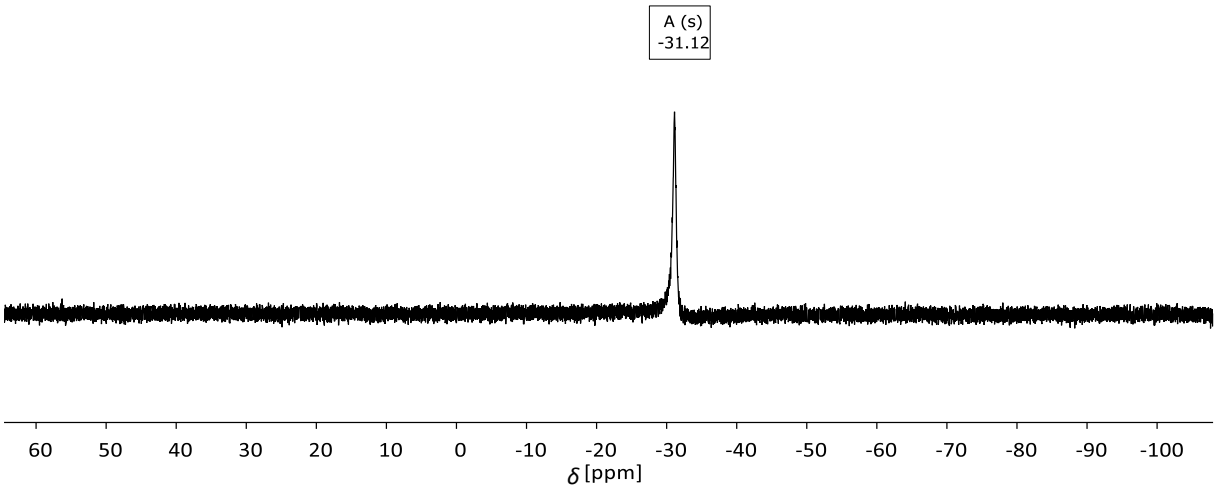

Figure S48 $^{31}P\{^{1}H\}$ NMR spectrum of a solution of 2,3,6,7,10,11-hexakis((benzo[*d*][1,3,2]dioxaborol-2-yl)ethynyl)-4b,8b,12b-tri-*n*-propyltribenzotriquinacene (**9**)·3 BisPhos in C_6D_6 (202 MHz, 293 K).

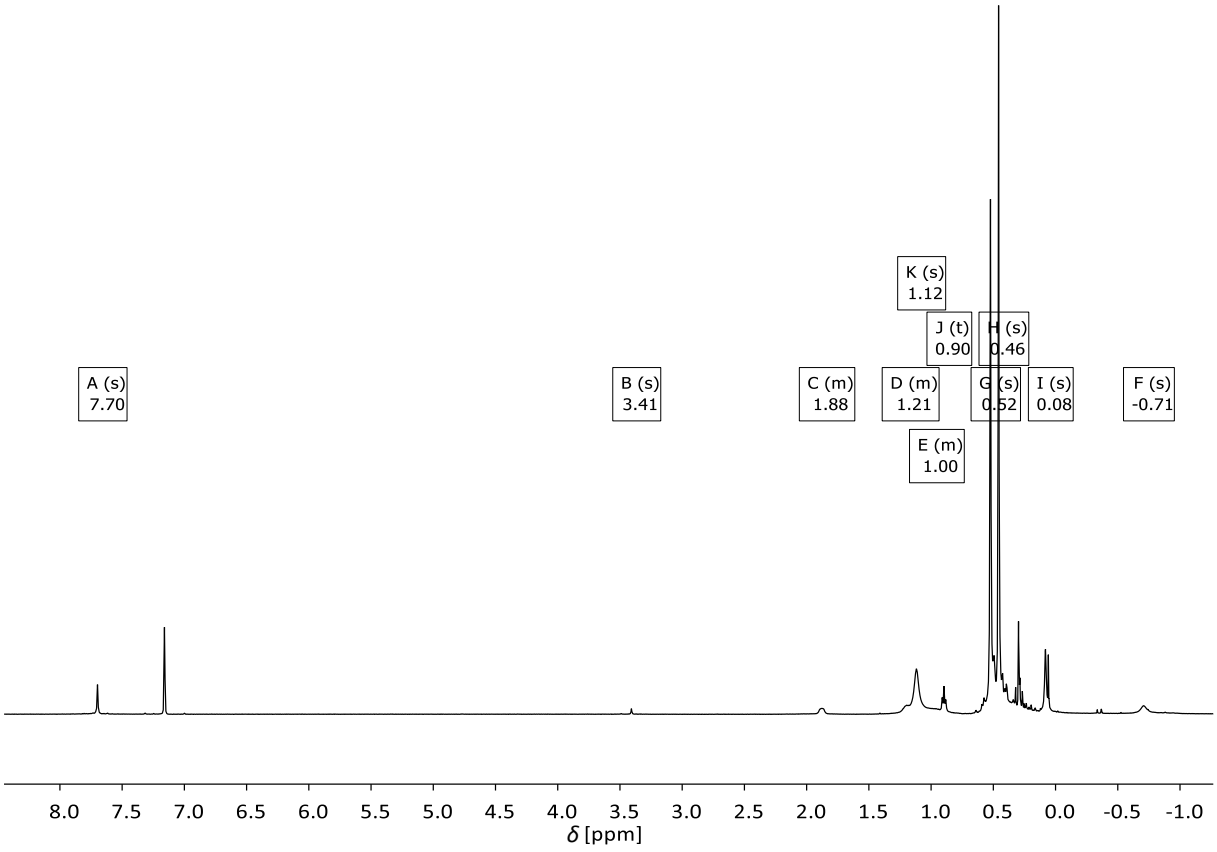

Figure S49 ^{1}H NMR spectrum of a solution of 2,3,6,7,10,11-hexakis(2-bis(bis(trimethylsilylmethyl)aluminyl)ethynyl)-4b,8b,12b-tri-*n*-propyltribenzotriquinacene (**10**)·3 BisPhos in C_6D_6 (500 MHz, 293 K).

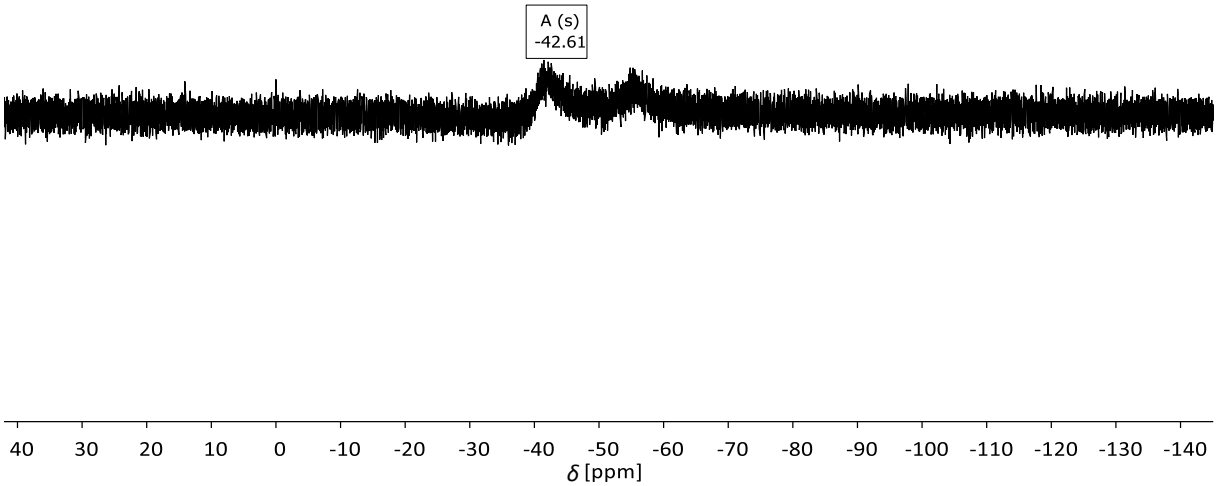

Figure S50 $^{31}P\{^{1}H\}$ NMR spectrum of a solution of 2,3,6,7,10,11-hexakis(2-bis(bis(trimethylsilylmethyl)aluminyl)ethynyl)-4b,8b,12b-tri-*n*-propyltribenzotriquinacene (**10**)·3 BisPhos in C_6D_6 (202 MHz, 293 K).

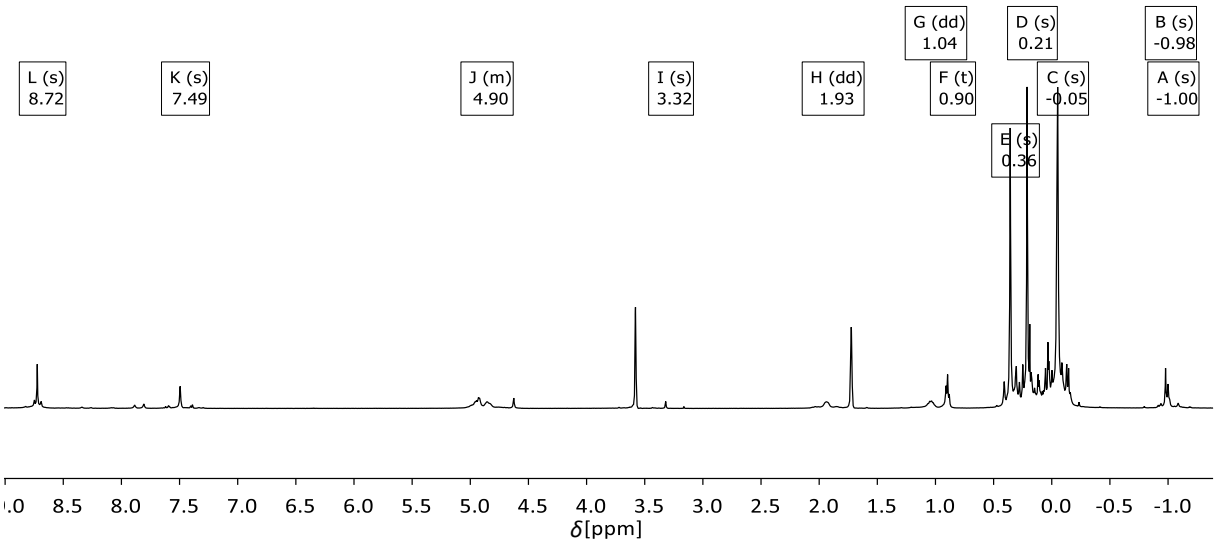

Figure S51 ^{1}H NMR spectrum of a solution of 2,3,6,7,10,11-hexakis(2-bis(bis(trimethylsilylmethyl)aluminyl)ethynyl)-4b,8b,12b-tri-*n*-propyltribenzotriquinacene (**10**)· 3 BisTriaz in THF-*d*8 (500 MHz, 293 K).

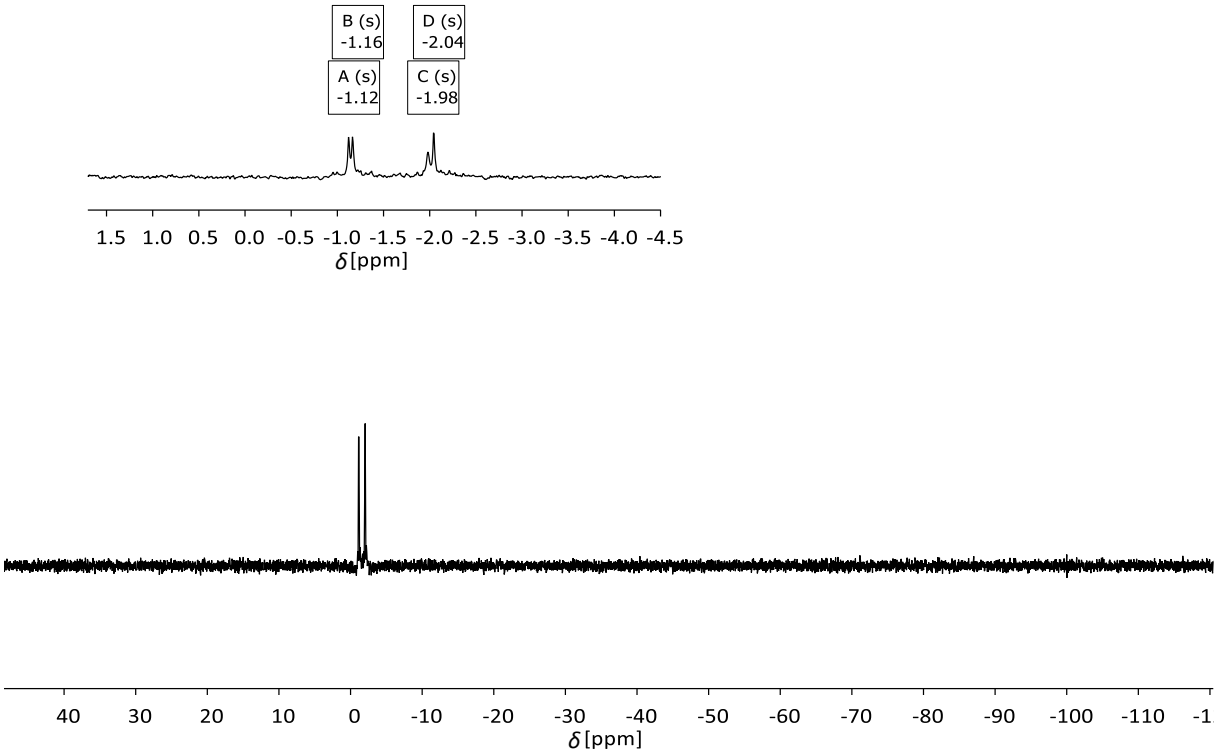

Figure S52 ^{1}H NMR spectrum of a solution of 2,3,6,7,10,11-hexakis(2-bis(bis(trimethylsilylmethyl)aluminyl)ethynyl)-4b,8b,12b-tri-*n*-propyltribenzotriquinacene (**10**)·3 BisTriaz in THF-*d*8 (99 MHz, 293 K).

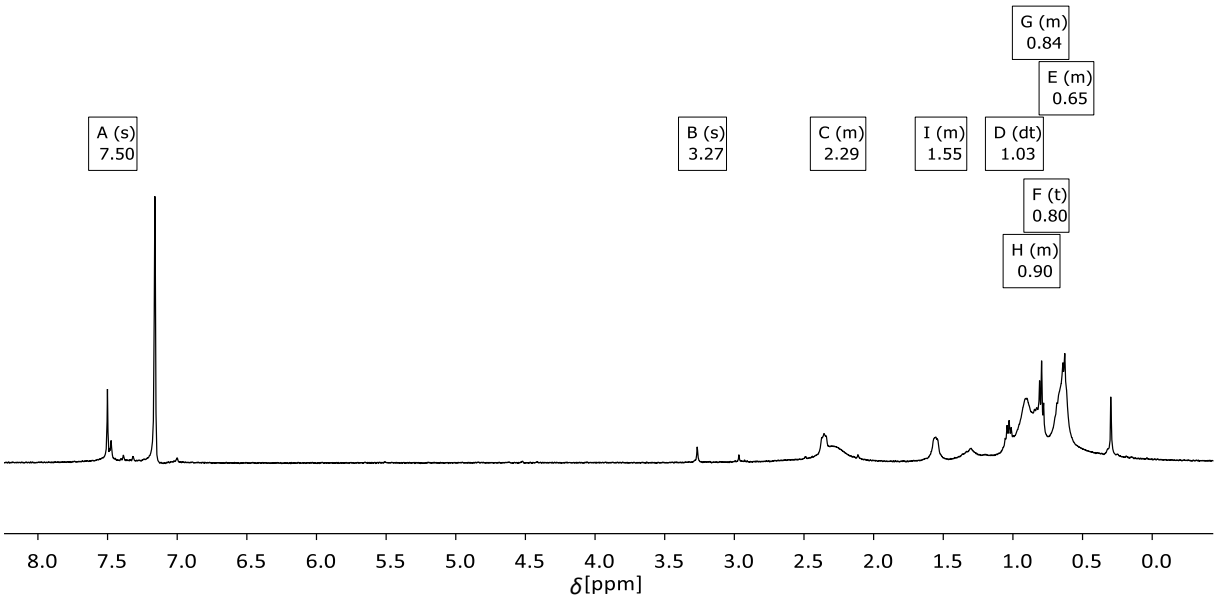

Fig S53 ^{1}H NMR spectrum of a solution of 2,3,6,7,10,11-hexakis((pentafluroethyl)stibanyl)ethynyl)-4b,8b,12b-tri-*n*-propyltribenzotriquinacene (**11**)·3 Bu_4NI in C_6D_6 (500 MHz, 293 K).

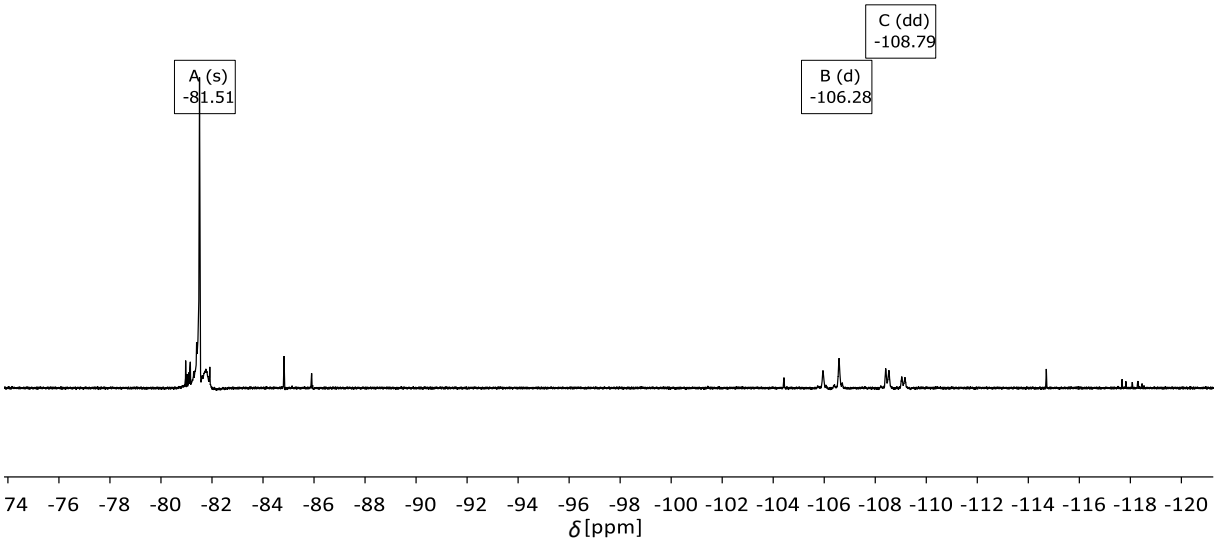

Fig S54 ^{19}F NMR spectrum of a solution of 2,3,6,7,10,11-hexakis((pentafluroethyl)stibanyl)ethynyl)-4b,8b,12b-tri-*n*-propyltribenzotriquinacene (**11**)·3 Bu_4NI in C_6D_6 (126 MHz, 293 K).

Crystallographic data

Suitable crystals were obtained by slow evaporation of saturated solutions in *n*-hexane (**2**, **4**) or toluene (**3**), by cooling saturated solutions of toluene (**7**, **8**) or *n*-hexane (**10**) to −30°C or slowly grown from supersaturated solutions in benzene (**10**·3 BisPhos). The crystals were selected, coated with PARATONE-N oil, mounted on a glass fibre and transferred onto the goniometer of the diffractometer into a cold nitrogen gas stream, which immediately solidifies the oil. Data collection was performed on a Rigaku SuperNova diffractometer. Using Olex2[1] the structures were solved with the SHELXT[2] structure solution program and refined with the SHELXL[3] refinement package.

CCDC 2325781-2325787 contain the supplementary crystallographic data for this paper. These data can be obtained free of charge from The Cambridge Crystallographic Data Centre via http://www.ccdc.cam.ac.uk/conts/retrieving.html

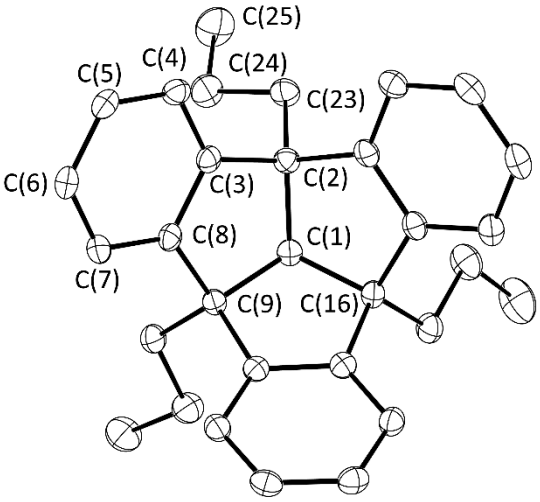

Figure S55 Molecular structure of **2** in the crystalline state. Displacements ellipsoids are drawn at 50% probability level. Hydrogen atoms are omitted for clarity. Selected bond lengths [Å] and angles [°]: C(1)–C(2) 1.565(2), C(2)–C(3) 1.523(2), C(3)–C(4) 1.395(2), C(4)–C(5) 1.394(2), C(2)–C(23) 1.541(2), C(23)–C(24) 1.524(2), C(24)–C(25) 1.529(2), C(1)–C(2)–C(3) 103.9(1), C(2)–C(3)–C(4) 127.9(1), C(3)–C(4)–C(5) 119.1(1).

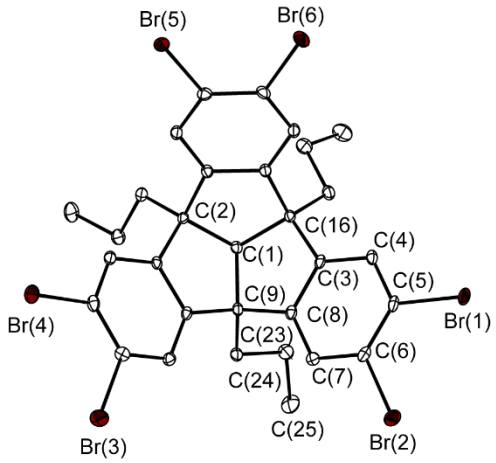

Figure S56 Molecular structure of **2** in the crystalline state. Displacements ellipsoids are drawn at 50% probability level. Hydrogen atoms are omitted for clarity. Selected bond lengths [Å] and angles [°]: C(1)–C(2) 1.568(3), C(2)–C(3) 1.522(4), C(3)–C(4) 1.395(3), C(4)–C(5) 1.391(4), C(5)–C(6) 1.390(4), C(5)–Br(1) 1.890(3) C(6)–C(7) 1.395(4), C(7)–C(8) 1.385(4), C(8)–C(9) 1.518(3), C(9)–C(23) 1.540(3), C(23)–C(24) 1.527(4), C(24)–C(25) 1.526(4), C(1)–C(2)–C(3) 103.6(2), C(2)–C(3)–C(4) 127.6(2), C(3)–C(4)–C(5) 119.2(2), C(1)–C(9)–C(23) 115.1(2), C(4)–C(5)–Br(1) 118.1(2).

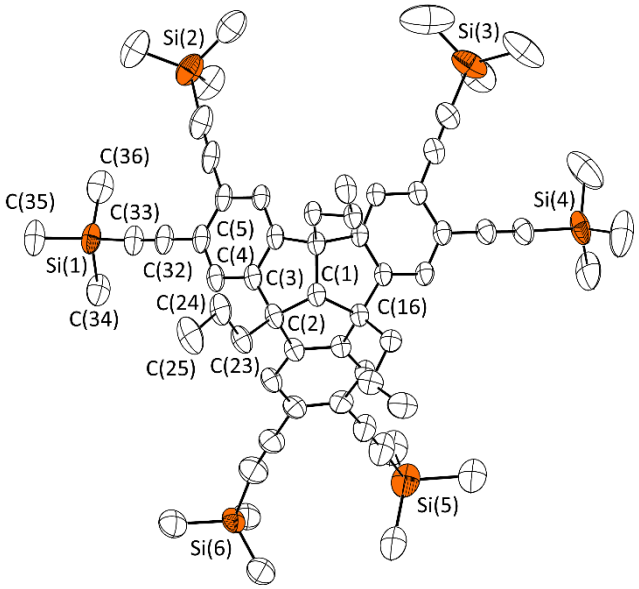

Figure S57 Molecular structure of **4** in the crystalline state. Displacements ellipsoids are drawn at 50% probability level. Hydrogen atoms and disordered parts are omitted for clarity. Selected bond lengths [Å] and angles [°]: C(1)–C(2) 1.569(4), C(2)–C(3) 1.513(4), C(3)–C(4) 1.396(4), C(4)–C(5) 1.397(5), C(2)–C(23) 1.536(4), C(23)–C(24) 1.515(5), C(24)–C(25) 1.522(5), C(5)–C(32) 1.433(4), C(32)–C(33) 1.209(4), Si(1)–C(33) 1.850(3), Si(1)–C(34) 1.873(4), C(1)–C(2)–C(3) 103.5(2), C(2)–C(3)–C(4) 127.6(3), C(3)–C(4)–C(5) 120.2(3), C(4)–C(5)–C(32) 120.9(3), C(5)–C(32)–C(33) 178.5(3), C(32)–C(33)–Si(1) 174.1(3), C(33)–Si(1))–C(34) 107.8(2).

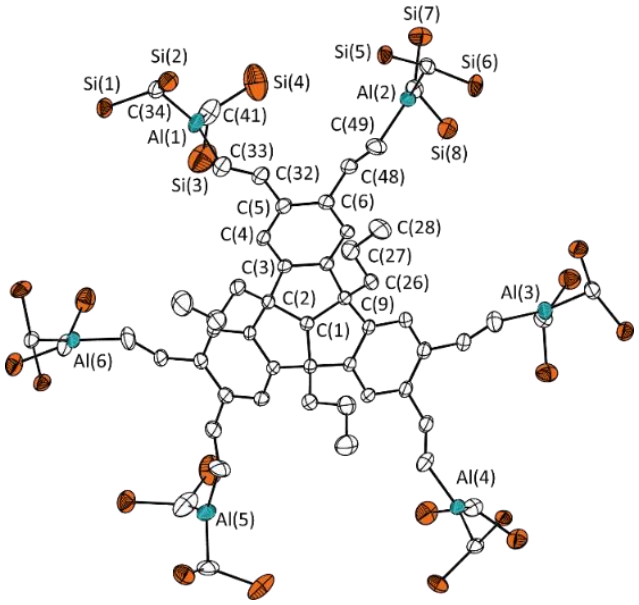

Figure S58 Molecular structure of **7** in the crystalline state. Displacement ellipsoids are drawn at 50% probability level. Methyl C atoms and H atoms as well as disordered atoms are omitted for clarity. Selected bond lengths [Å] and angles [°]: C(1)–C(2) 1.560(3), C(2)–C(3) 1.649(4), C(3)–C(4) 1.426(4), C(4)–C(5) 1.509(4), C(5)–C(32) 1.518(4), C(32)–C(33) 1.322(4), Al(1)–C(33) 2.001(4), Al(1)–C(34) 1.937(3), C(1)–C(2)–C(3) 105.3(2), C(2)–C(3)–C(4) 131.2(2), C(3)–C(4)–C(5) 124.6(2), C(4)–C(5)–C(32) 124.2(2), C(5)–C(32)–C(33) 124.9(3), C(32)–C(33)–Al(1) 121.4(3), C(33)–Al(1))–C(34) 116.4(2), C(33)–Al(1))–C(41) 124.2(2), C(34)–Al(1))–C(41) 119.4(2).

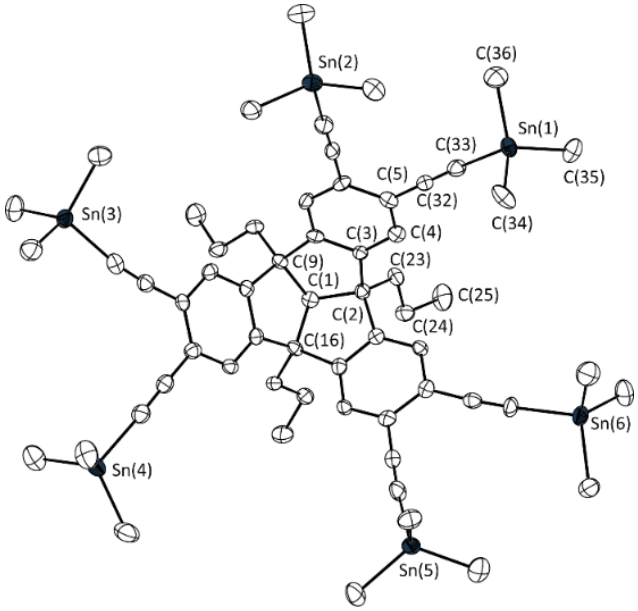

Figure S59 Molecular structure of **8** in the crystalline state. Displacement ellipsoids are drawn at 50% probability level. Hydrogen atoms are omitted for clarity. Selected bond lengths [Å] and angles[°]: C(1)–C(2) 1.573(10), C(2)–C(3) 1.507(10), C(3)–C(4) 1.396(10), C(4)–C(5) 1.383(11),), C(2)–C(23) 1.576(11), C(23)–C(24) 1.516(11), C(24)–C(25) 1.531(12), C(5)–C(32) 1.419(11), C(32)–C(33) 1.209(11), Sn(1)–C(33) 2.125(8), Sn(1)–C(34) 2.128(9); C(1)–C(2)–C(3) 103.9(6), C(2)–C(3)–C(4) 128.1(7), C(3)–C(4)–C(5) 121.6(7), C(4)–C(5)–C(32) 121.8(7), C(5)–C(32)–C(33) 178.6(9), C(32)–C(33)–Sn(1) 173.5(8), C(33)–Sn(1))–C(34) 103.8(3).

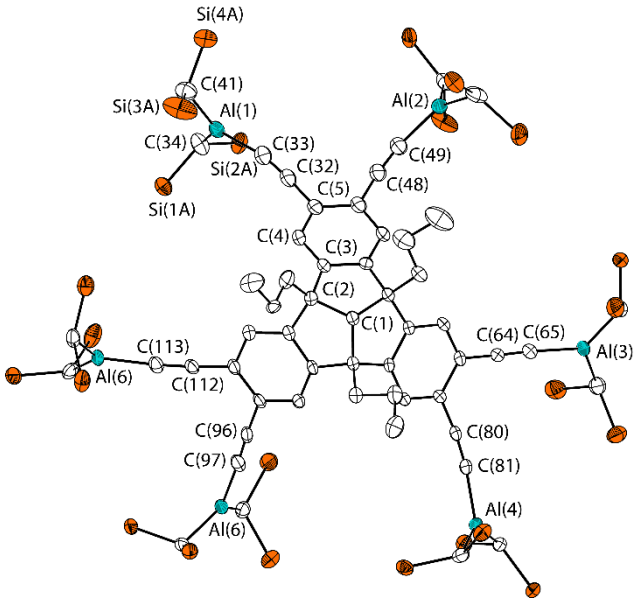

Figure S60 Molecular structure of **10** in the crystalline state. Displacement ellipsoids are drawn at 50% probability level. Hydrogen atoms and methyl C atoms as well as disordered parts are omitted for clarity. For further details, see the ESI.† Selected bond lengths [Å] and angles [°]: C(1)–C(2) 1.568(5), C(2)–C(3) 1.520(6), C(3)–C(4) 1.393(6), C(4)–C(5) 1.386(6), C(5)–C(32) 1.444(6), C(32)–C(33) 1.199(6), Al(1)–C(33) 1.903(5), Al(1)–C(34) 1.932(4), Al(1)–C(41) 1.945(5); C(1)–C(2)–C(3) 103.0(3), C(32)–C(33)–Al(1) 168.4(4), C(33)–Al(1)–C(34) 118.8(2), C(33)–Al(1)–C(41) 118.9(2), C(48)–C(49)–Al(2) 165.0(4). C(80)–C(81)–Al(4) 166.7(3), C(96)–C(97)–Al(5) 176.7(4), C(112)–C(113)–Al(6) 170.7(4).

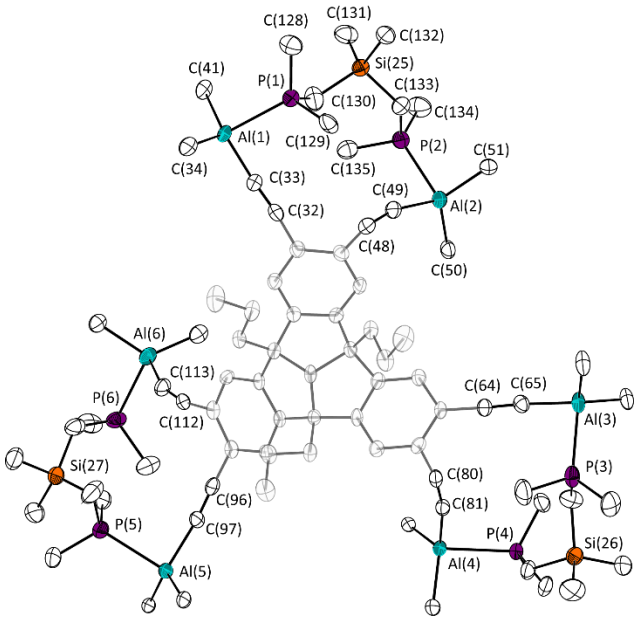

Figure S61 Molecular structure of **10**·(3 BisPhos) in the crystalline state. Displacement ellipsoids are drawn at 50% probability level. Hydrogen atoms as well as the $SiMe_3$ groups are omitted and the TBTQ backbone is greyed out for clarity. Selected bond lengths [Å] and angles [°]: C(32)–C(33) 1.210(6), Al(1)–C(33) 1.973(7), Al(1)–C(34) 1.977(8), Al(1)–C(41) 2.025(10), Al(1)–P(1) 2.506(7), P(1)–C(130) 1.866(6), C(130)–Si(25) 1.890(6),); C(32)–C(33)–Al(1) 156.4(5), C(33)–Al(1)–P(1) 89.7(2), C(33)–Al(1)–C(34) 111.2(4), C(33)–Al(1)–C(41) 123.5(4), Al(1)–P(1)–C(128) 119.9(3), C(48)–C(49)–Al(2) 164.0(4). C(80)–C(81)–Al(4) 163.2(4), C(112)–C(113)–Al(6) 160.3(4).

Table S1 Crystallographic data of TBTQ compounds **2**, **3**, and **4**.

	2[a]	**3**[b]	**4**[c]
Empirical formula	$C_{31}H_{34}$	$C_{72.5}H_{68}Br_{12}$	$C_{82}H_{102}Si_6$
M_r	406.58	1898.19	1256.17
T [K]	100.0(1)	100.0(1)	100.0(1)
Crystal system	triclinic	monoclinic	monoclinic
Space group	$P\bar{1}$	$P2_1/n$	$I2/a$
a [Å]	9.0140(4)	19.0157(3)	27.3971(4)
b [Å]	9.3643(3)	20.0868(4)	25.3293(3)
c [Å]	14.7850(5)	19.9871(3)	24.4731(3)
α [°]	99.294(3)	90	90
β [°]	104.180(3)	113.226(2)	99.9320(10)
γ [°]	93.662(3)	90	90
V [Å^3]	1187.09(8)	7015.6(2)	16728.6(4)
Z	2	4	8
ρ_{calc} [g cm^{-3}]	1.137	1.797	0.998
μ [mm^{-1}]	0.473	6.892	1.208
F(000) [e]	440	3692	5424
Crystal size [mm^3]	0.12 × 0.08 × 0.02	0.22 × 0.077 × 0.062	0.24 × 0.17 × 0.16
Radiation [Å]	Cu Kα (λ = 1.54184)	Mo Kα (λ = 0.71073)	Cu Kα (λ = 1.54184)
2Θ range for data collection [°]	6.272 to 152.684	3.004 to 64.402	4.784 to 153.436
Index ranges	$-11 \le h \le 11$, $-6 \le k \le 11$, $-18 \le l \le 18$	$-28 \le h \le 26$, $-28 \le k \le 28$, $-29 \le l \le 28$	$-34 \le h \le 31$, $-31 \le k \le 31$, $-30 \le l \le 30$
Reflections collected	9704	105349	166256
Independent reflections	4856 [R_{int} = 0.0228, R_{sigma} = 0.0333]	22899 [R_{int} = 0.0485, R_{sigma} = 0.0461]	17424 [R_{int} = 0.0329, R_{sigma} = 0.0144]
Reflections with $I > 2\sigma(I)$	4125	17003	15581
Data/restraints/parameters	4856/0/416	22899/164/801	17424/157/709
Goodness-of-fit on F^2	1.037	1.015	1.046
Final R indexes [$I > 2\sigma(I)$]	R_1 = 0.0419, wR_2 = 0.1037	R_1 = 0.0388, wR_2 = 0.0732	R_1 = 0.0979, wR_2 = 0.2880
Final R indexes [all data]	R_1 = 0.0508, wR_2 = 0.1109	R_1 = 0.0661, wR_2 = 0.0818	R_1 = 0.1033, wR_2 = 0.2938
Largest diff. peak/hole [e Å^{-3}]	0.35/−0.21	1.47/−1.05	0.81/−0.73
CCDC number	2325781	2325782	2325783

[a] Hydrogen atoms were refined isotropically.

[b] Disorder of a half toluene molecule on an inversion centre. This toluene was included using the fragment database of Olex2. The anisotropic displacement parameters were restrained with ISOR.

[c] Disorder over two sites of C(39), C(40), C(41) (57:43), of C(54), C(55), C(56) (54:46) and of Si(6), C(59), C(60), C(61) (66:34). Displacement parameter were restrained with RIGU. Solvent molecules were disordered. A solvent mask was calculated, and 1258 electrons were found in a volume of 5420 Å^3 in 2 voids. This is consistent with the presence of 2.5 C_6H_6, 1 C_6H_6 per formula unit, which accounts for 1176.0 electrons.

Table S2 Crystallographic data of TBTQ compounds **7**, **8**, **10** and **10**·(3 BisPhos) .

	7[a]	**8**	**10**[b]	**10**·(3 BisPhos)[c]
Empirical formula	$C_{155}H_{300}Al_6Si_{24}$	$C_{89}H_{114}Sn_6$	$C_{139}H_{284}Al_6Si_{24}$	$C_{181}H_{352}Al_6P_6Si_{27}$
M_r	2999.97	1895.94	2791.69	3634.73
T [K]	100.0(1)	100.0(1)	100.0(1)	100.0(1)
Crystal system	monoclinic	monoclinic	triclinic	triclinic
Space group	$C2/c$	$P2_1/c$	$P\bar{1}$	$P\bar{1}$
a [Å]	39.1993(6)	28.3182(9)	17.4659(5)	25.0396(4)
b [Å]	22.8491(2)	25.1639(5)	21.6812(6)	25.2861(5)
c [Å]	46.9723(7)	25.1299(7)	26.9593(8)	28.1063(5)
α [°]	90	90	105.168(2)	95.762(1)
β [°]	109.4807(16)	97.566(3)	93.414(2)	106.883(2)
γ [°]	90	90	105.343(2)	118.836(2)
V [Å^3]	39663.2(9)	17751.6(8)	9410.8(5)	14290.2(5)
Z	8	8	2	2
ρ_{calc} [g cm^{-3}]	1.005	1.419	0.985	0.845
μ [mm^{-1}]	1.991	1.701	0.225	0.203
F(000) [e]	13152	7584	3064	3968
Crystal size [mm^3]	0.18 × 0.1 × 0.02	0.191 × 0.096 × 0.053	0.26 × 0.21 × 0.08	0.425 × 0.228 × 0.187
Radiation [Å]	Cu Kα (λ = 1.54184)	Mo Kα (λ = 0.71073)	Mo Kα (λ = 0.71073)	Mo Kα (λ = 0.71073)
2Θ range for data collection [°]	4.546 to 179.294	3.236 to 51.364	6.602 to 50.7	6.426 to 50.054
Index ranges	–47 ≤ h ≤ 49, –28 ≤ k ≤ 19, –60 ≤ l ≤ 60	–34 ≤ h ≤ 34, –30 ≤ k ≤ 30, –30 ≤ l ≤ 30	–21 ≤ h ≤ 21, –26 ≤ k ≤ 26, –32 ≤ l ≤ 32	–29 ≤ h ≤ 29, –30 ≤ k ≤ 30, –33 ≤ l ≤ 33
Reflections collected	171495	158656	158906	598233
Independent reflections	40324 [R_{int} = 0.0588, R_{sigma} = 0.0372]	33709 [R_{int} = 0.0848, R_{sigma} = 0.0726]	34364 [R_{int} = 0.0620, R_{sigma} = 0.0655]	50346 [R_{int} = 0.0805, R_{sigma} = 0.0397]
Reflections with I > 2σ(I)	33297	23036	24611	36173
Data/restraints/parameters	40322/1514/1769	33709/0/1753	34364/1907/1947	50346/31/1974
Goodness-of-fit on F^2	1.047	1.099	1.064	1.060
Final R indexes [I > 2σ(I)]	R_1 = 0.0705, wR_2 = 0.1877	R_1 = 0.0593, wR_2 = 0.1405	R_1 = 0.0755, wR_2 = 0.1703	R_1 = 0.0831, wR_2 = 0.2255
Final R indexes [all data]	R_1 = 0.0808, wR_2 = 0.1972	R_1 = 0.1006, wR_2 = 0.1621	R_1 = 0.1088, wR_2 = 0.1872	R_1 = 0.1115, wR_2 = 0.2542
Largest diff. peak/hole [e Å^{-3}]	0.97/−0.62	2.25/−1.27	1.94/−0.69	0.78/−0.48
CCDC number	2325784	2325785	2325786	2325787

[a] A solvent mask was calculated and 1556 electrons were found in a volume of 7628 Å^3 in 6 voids per unit cell. This is consistent with the presence of 4 toluene molecules per asymmetric unit which account for 1600 electrons per unit cell. Disorder of $(Bis)_2Al$-groups over two sites: Si(1), Si(2), C(35), C(36), C(38) C(40) (91:9); Si(3), C(42) to C(47) (61:39); C(93) to C(95) (78:22); Si(17); Si(18), C(98) to C(102) (59:41); Si(19), Si(20), C(106) to C(111) (68:32); C(123) to C(124) (63:47). Suitable constraints and restraints were used.

[b] Disorder of some parts of the molecule over two sites with a ratio of 63:37 Disorder of one hexane molecule over two sites with a ratio of 75 (C128–C133):25 (C140–C145).

[c] Disorder over to sites of Si(3) to Si(8), Si(25), Al(1), P(1), P(2), C(41) to C(47), C(50) to C(59), C(61), C(63), C(129), C(131) to C(136) (82:20), Si(12); C(77) to C(79) in ratio (90:10), Si(27), C(147), C(148) (88:12), Si(21), Si(22), C(114) to C(120) (80:20). The ADP's of the disordered atoms were constrained to be same in pairs. Solvent C_6H_6 was disordered and partially occupied, therefore a solvent mask was calculated and 433 electrons were found in a volume of 5445 Å^3 in 4 voids per unit cell. This is consistent with the presence of 5 C_6H_6 per asymmetric unit which account for 420 electrons per unit cell.

References

1. O. V. Dolomanov, L. J. Bourhis, R. J. Gildea, J. A. K. Howard and H. Puschmann, *J. Appl. Crystallogr*., 2009, **42**, 339−341.
2. (a) G. M. Sheldrick, *Acta Crystallogr., Sect. A* 2008, 64, 112−122, (b) G. M. Sheldrick, *Acta Crystallogr*., *Sect. A* 2015, **71**, 3−8.
3. G. M. Sheldrick, *Acta Crystallogr*., *Sect. C* 2015, **71**, 3−8.